SEMMELWEIS EGYETEM

DOKTORI ISKOLA

Ph.D. értekezések

3371.

BÁRDOS VIVIEN

A gyógyszerészeti tudományok korszerű kutatási irányai

című program

Programvezető: Dr. Antal István, egyetemi tanár

Témavezetők: Dr. Takácsné Dr. Novák Krisztina, egyetemi tanár

Dr. Angi Réka, egyetemi adjunktus

THE IMPACT OF FORMULATION EXCIPIENTS ON SOLUBILITY AND PERMEABILITY DETERMINED BY SMALL-SCALE IN VITRO METHODS

PhD thesis

Vivien Bárdos

Semmelweis University Doctoral School

Pharmaceutical Sciences and Health Technologies Division

Supervisor:	Krisztina Takács-Novák, D.Sc.
Co-supervisor:	Réka Erzsébet Angi, Ph.D.
Official reviewers:	Dr. Berkó Szilvia, Ph.D. Dr. Kállai-Szabó Nikolett, Ph.D.

Head of the Complex Examination Committee:
István Antal, Ph.D.

Members of the Complex Examination Committee:
Krisztina Ludányi, Ph.D.
Zsuzsanna Rozmer, Ph.D.

Budapest
2025

Table of Contents

List of Abbreviations

ADME – Absorption, Distribution, Metabolism, and Excretion

AI – Artificial Intelligence

APIs – Active Pharmaceutical Ingredients

BBB – Blood-Brain Barrier

BCS – Biopharmaceutical Classification System

BRB – Britton-Robinson buffer

CaCo-2 – Caucasian Colon Adenocarcinoma

CADD – Computer-Aided Drug Design

CAR – Carbamazepine

CDs – Cyclodextrins

CMC – Critical Micelle Concentration

D-P – Dissolution-permeation

DS-PAMPA – Double-Sink PAMPA

DTT – Dissolution Template Titration

FaSSIF – Fasted-state simulated intestinal fluid

FeSSIF – Fed-state simulated intestinal fluid

GI – Gastrointestinal

HH – Henderson-Hasselbalch

HLB – Hydrophilic-lipophilic balance

HPβCD – Hydroxypropyl-β-cyclodextrin

HTS – High Throughput Screening

IVIVC – *in vitro-in vivo* correlation

K_p – Permeability coefficient

LBFs – Lipid-based formulations

MDCK – Madin-Darby Canine Kidney

NAP – Naproxen

P_m – Membrane permeability

PAMPA – Parallel Artificial Membrane Permeability Assay

PER – Phenylethyl resorcinol

PIMO – Pimobendan

PVDF – Polyvinylidene fluoride

PVP-K25 – Polyvinylpyrrolidone-K25

PVPVA 64 – Polyvinylpyrrolidone/vinyl acetate 64

QSAR – Quantitative Structure-Activity Relationships

SBEβCD – Sulfobutyl-ether-β-cyclodextrin

SD – Standard Deviation

SDs – Solid dispersions

SLS – Sodium Lauryl Sulfate

SSF – Saturation Shake-Flask

TDDSs – Transdermal Drug Delivery Systems

TEWL – Trans-Epidermal Water Loss

UWL – Unstirred Water Layer

1. Introduction

Pharmaceutical research aims to discover and develop novel therapeutic agents that are effective, safe, and of high quality. The complex nature of drug development renders the process typically long-lasting, costly, and carries a high risk of failure. Consequently, the industry continuously seeks to adopt innovative technologies and methodologies to improve development outcomes.

The paradigm of drug discovery has altered significantly in recent decades. Since the 1960s, empirical methods – like botanical extractions and random compound screening – have been replaced by the novel approach of rational drug design. The first method, the Quantitative Structure-Activity/Property Relationships (QSAR/QSPR) analysis was based on the investigation of structure-activity or property relationships [1]. For more effectiveness this method was supplemented with a 3D molecular modelling and computer-aided design (Computer Aided Drug Design, CADD) [2]. In the 1990s, the number of new active compounds increased with the rise of high-throughput screening (HTS) techniques and combinatorial chemistry, which revolutionized hit identification and lead optimization. The next paradigm-change can be attributed to the human genome project, where the identification of the mechanisms and the possible targets of diseases came into focus [3,4]. Currently, the influence of artificial intelligence (AI) is expected to improve the efficiency of drug discovery and decrease the risk of late-stage failures by offering early predictions regarding novel chemical and biological targets. AI also facilitates drug repurposing by identifying novel indications for existing compounds [5].

A persistent challenge in drug development is poor aqueous solubility, as it affects approximately 40% of commercial drugs and 70-90% of new drug candidates [6]. This emphasizes the importance of early-stage physicochemical profiling, which includes the examination of acid-base properties, stability, solubility, lipophilicity and permeability of the drug candidate for optimal bioavailability. This is completed by pharmaceutical profiling to investigate ADME characteristics, drug interactions, and safety profiles to enhance development efficiency.

As a result, various solubility-enhancing techniques have been applied in both original and generic drug research and development. However, since solubility and permeability are consecutive processes, formulation strategies must be evaluated for their impact on both parameters to ensure adequate bioavailability. This necessity has led to

academic, regulatory and industrial collaborations, such as, OrBiTo (Oral Biopharmaceutics Tool) [7], and UNGAP (Understanding Gastrointestinal Absorption-related Processes) [8]. These consortiums aim to develop and validate *in vitro* and *in silico* models to enhance the understanding of gastrointestinal drug absorption, improve the *in vitro-in vivo* correlation (IVIVC), and optimize the efficiency of drug development processes.

1.1. Routes of drug administration

Drugs can be administered via various routes, including oral, intravenous, subcutaneous, inhalational, intranasal, and transdermal pathways, to mention the most important ones. The selection of the appropriate route can be affected by many factors such as the type of the disease, the status of the patient (e.g. consciousness level), and whether a localized or systemic effect is desired. Each route presents specific benefits and drawbacks [9]. The most widely used route remains the oral administration, while the transdermal drug delivery systems have been developing dynamically in recent times. Thus, in the following, focusing on the topics of the dissertation, only the oral and transdermal drug delivery will be discussed in detail.

1.1.1. Oral administration

The most common route is the oral administration due to its non-invasive nature, cost-effectiveness, ease of dosing, and high patient compliance [10,11]. Although there are some major limitations, such as first-pass metabolism and the acidic medium of the stomach, which on one hand can decompose some compounds before absorption, and on the other hand can cause solubility problems for many drugs [9].

During oral administration, the bioavailability of a compound can be described by the LADME process. Liberation, the release of the drug from the dosage form, affects the onset of the drug's action. Then comes absorption through membranes to reach the bloodstream, followed by distribution, metabolism, and excretion [12].

The schematic illustration of the GI tract is shown in Fig. 1. The stomach and the small intestine play dominant roles in the absorption of orally administered drugs. In the case of drug molecule transport the mucosal layer of the lumen of the GI system plays a significant role [13].

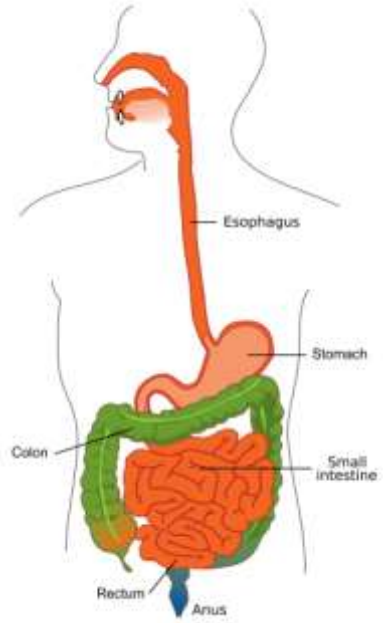

Figure 1. The schematic illustration of GI tract [14]

However, in the case of absorption, the composition and the pH of the GI media, and the transit time are also key factors. The stomach has a highly acidic medium (pH 1.0-3.5), due to the hydrochloric acid secreted by the parietal cells. This medium may favour the absorption of acidic substances, yet it can also cause the degradation of APIs. Pepsin secretion also occurs, which plays an important role in the digestion of proteins into smaller peptides, but thereby limits the oral administration of certain molecules. Furthermore, gastric emptying takes around 2 h but is highly dependent on the physical form of the drug formulation (e.g. pellet or tablet) [15,16]. The small intestine's higher pH (*duodenum* pH 4.0-5.5; *jejunum* pH 5.5-7.0; *ileum* pH 7.0-7.5) is more favourable for the absorption of basic molecules. The microvilli provide a larger surface area, and the presence of bile salts and lecithin results in a better solubilization of the compounds, which contributes to better absorption. Its longer transit time (~3-4 h) is also more suitable for absorption [10,11]. Food also has an influencing effect. In the case of the fed stomach the pH and the gastric emptying time can increase, whereas the pH of the small intestine will be decreased after a meal. The quality of the food also affects the secretion of bile salts and digestive enzymes.

During oral administration, the APIs must be dissolved in gastric fluid for absorption and to achieve an adequate receptor response. Furthermore, adequate lipophilicity is necessary for membrane permeation [3,17].

The work of *Amidon et al.* has emphasized how solubility and permeability are key factors in the relationship between the *in vitro* dissolution and the *in vivo* bioavailability of a drug [18]. The Biopharmaceutical Classification System (BCS) classified the APIs based on these two parameters. BCS I. molecules have high aqueous solubility and GI permeability, while BCS II. compounds are characterized by good permeability but low solubility. BCS III. APIs are highly soluble yet poorly permeable, while those belonging to BCS IV. have low solubility as well as low permeability [18,19].

1.1.2. Transdermal application

Transdermal drug delivery systems (TDDSs) are a dynamically developing route of administration in recent years. Transdermal delivery has several advantages, such as its non-invasive nature, avoiding first-pass metabolism, bypassing the gastrointestinal (GI) system, and resulting in a stable blood level. However, a significant limitation is that not all active pharmaceutical ingredients (APIs) possess the appropriate physicochemical properties required for effective transdermal transport, such as adequate lipophilicity, low molecular weight, and neutral character [20–22].

Its prominence as a route of drug administration is attributed to the fact that the skin, as the largest organ in the human body (with approximately 2 m^2 area) possesses a rich blood supply, making it an ideal surface for absorption. However, it also serves as a significant barrier to foreign substances. The pH of the healthy skin is slightly acidic (pH 4.1-5.8). This contributes to the barrier function by inhibiting the growth of harmful bacteria (like *Staphylococcus aureus*) and fungi. The exact value depends on the body part, the age and the different skincare products that are potentially used [23]. The skin contains 3 layers: the epidermis, dermis, and hypodermis (Fig. 2.).

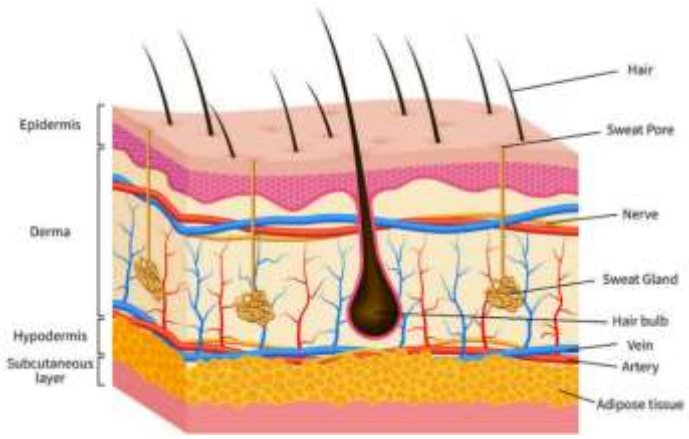

Figure 2. The structure of skin

(http://thedermspecs.com/blog/skin-anatomy-101/)

The epidermis consists of 5 parts: the *stratum corneum, stratum lucidum, stratum granulosum, stratum spinosum*, and *stratum basale*. The *stratum corneum* serves as a primary barrier against the transdermal penetration of most pharmaceutical compounds and exogenous substances. This protective function arises from the tightly packing of hydrophilic keratin proteins alongside hydrophobic lipids arranged in lamellae. The major components contributing to its hydrophobicity are ceramides (50%), cholesterol (25%), fatty acids, etc. The dermis primarily provides elasticity and strength, and the blood vessels run here. Below it, the hypodermis consists primarily of adipose tissue, which contributes to thermoregulation, mechanical protection, and facilitates neural and vascular transmission [21,24,25].

Enhancing drug permeation across the *stratum corneum* is therefore a key focus in the development of effective TDDSs.

The first generation of TDDSs includes creams, ointments, gels, and patches, where the *stratum corneum's* barrier function and the physicochemical properties of the drug can limit the effectiveness of the administration. The following TDDSs applied several permeability enhancing methods to increase the penetration across the *stratum corneum*. This can be reached by physical methods like iontophoresis, where electric current is applied as the driving force or microneedles, which create a microchannel for the drug delivery by disrupting the *stratum corneum*. Another option for permeability increasing is the application of chemical methods, such as microemulsions or several nanodelivery systems, like solid lipid nanoparticles or nanostructured lipid carriers [21,22,24,26].

1.2. Factors affecting absorption and bioavailability

As mentioned above, the optimal bioavailability is affected by biological barriers, such as the pH of the compartment or the transit time, and the physicochemical properties of the molecule (pK_a, solubility, log$P$, permeability) [3,11].

The various biological membranes serve as the primary barrier to permeation during absorption. Structurally, the membrane is a lipid bilayer formed by amphiphilic lipids and cholesterol in aqueous media [27]. The different APIs can be absorbed via passive or active transport. If a molecule is highly lipophilic, passive transport can take place across the cell (transcellularly); if it is small and hydrophilic, transport may occur paracellularly. If the molecule is a substrate for a transporter, it can enter the cell through active transport. Efflux transporters transport xenobiotics out of the cell, reducing the risk of toxicity [28]. Endocytosis is another possible way for the absorption of large and polar molecules. During this process the compounds can be engulfed by the cell membrane, forming vesicles. Key types of endocytosis include phagocytosis (cellular uptake of large particles), pinocytosis (cellular uptake of fluids and solutes), and receptor-mediated endocytosis (selective uptake of specific molecules) (Fig.3.) [29].

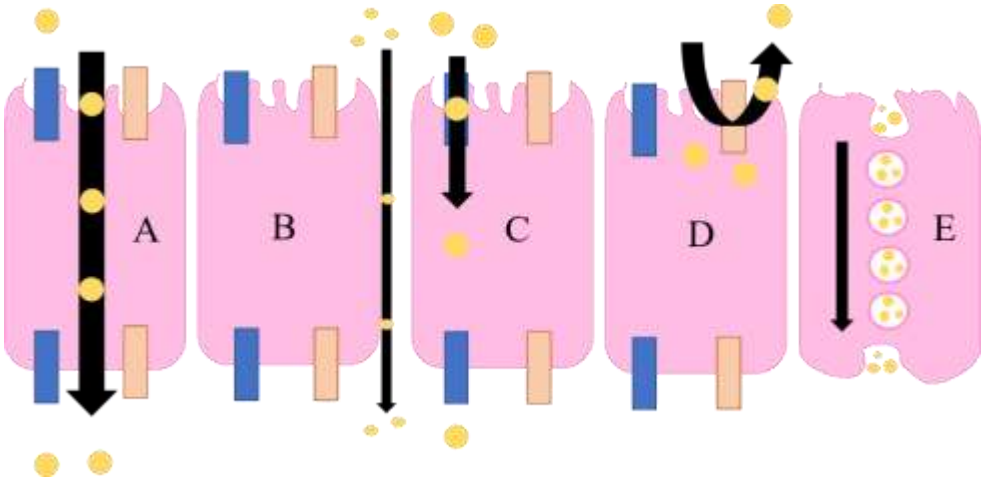

Figure 3. A: transcellular transport B: paracellular transport, C: influx, D: efflux, E: endocytosis

In the following, some important properties of the APIs in terms of absorption and bioavailability are presented.

Acid-base property

The majority of APIs possess ionizable functional groups. The acid-base properties can be characterized by the negative logarithm of the acid dissociation constant (pK_a). The ratio of the charged and uncharged form depends on the pK_a of the molecule and the pH of the GI compartment. When pH equals pK_a, 50% of the compound is in ionized and 50% of the compound is in unionized form. The knowledge of the ionization state is essential to optimize absorption. As the uncharged species is more lipophilic, it is the transport form that can be absorbed from the GI tract, while ionic interactions play an important role in receptor binding; therefore, the ionized form is essential for adequate effect (Fig. 4.).

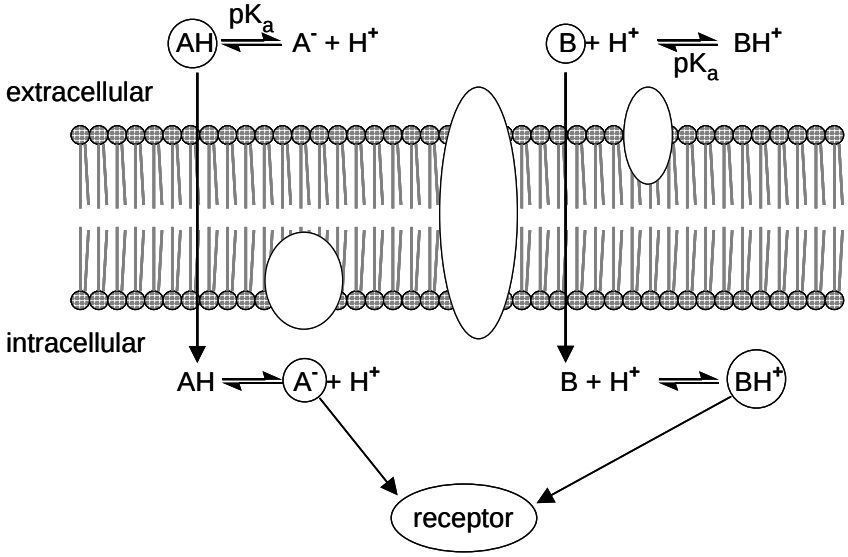

Figure 4. Transport and receptor forms of an acid and a base [3]

Lipophilicity

Lipophilicity, expressed as the octanol-water partition coefficient (*P*), is an important physicochemical parameter in the ADME process, influencing the membrane permeability and solubility of an API, as well as affecting their metabolism and pharmacokinetics [30]. It is usually characterized by the logarithm of the partition coefficient (log*P*). Also, log*P* describes the distribution of a uniformly charged – typically the neutral – species, so it is independent of the pH. The distribution coefficient *D*, which *is* influenced by pH, is utilized for ionizable compounds [3].

Metabolic stability and Drug-drug interactions

The sub-optimal bioavailability is primarily due to two key factors: metabolic instability and drug-drug interactions, especially when the interaction involves the inhibition or induction of cytochrome P450 enzymes.

Hepatic metabolism is the primary elimination mechanism for most drugs. As a result, it determines the clearance, the elimination half-life of the molecule and therefore the dosing frequency. Also, the plasma and the cells contain enzymes, such as esterase, which convert drugs [31,32].

In addition to the previously discussed properties, solubility and permeability are also key parameters for appropriate bioavailability, thus they will be presented in detail in the following chapters.

1.3. Solubility

Solubility is defined as the concentration of the saturated solution. It is important to note that solubility can be described in different ways, including the following terms.

1.3.1. Types of solubility

Equilibrium (thermodynamic) solubility (S)

Thermodynamic solubility is the concentration of a saturated solution in a heterogeneous system, where solid and solute are at equilibrium. In this state, the solid is present in excess. The thermodynamic solubility value is a characteristic molecular parameter of a substance that is constant at a given pressure and temperature [33–35].

Intrinsic solubility (S_0)

Intrinsic solubility was established because the thermodynamic solubility of ionizable compounds varies with pH. The intrinsic solubility is the equilibrium solubility of an ionizable compound at a pH value where it is in completely neutral (unionized or chargeless) form [36,37].

Kinetic solubility (S^{APP})

Kinetic solubility refers to the concentration of a solute at the initial point of precipitation. Since the system has not achieved the equilibrium, the kinetic solubility exceeds the thermodynamic value. During kinetic solubility experiments, the compound is introduced to the buffer in a concentrated (usually organic) solution form. There is a

significant risk of supersaturation in the aqueous solvent, after which precipitation of an amorphous or metastable crystalline form may occur, followed by crystalline precipitation [36].

1.3.2. Factors affecting solubility

Equilibrium solubility can be affected by various factors, such as pH, ionic strength, components of the medium, or the crystalline form, and particle size of the compound, which should be considered during the drug formulation process. These factors are listed below.

pH

The majority of drug molecules contain ionizable functional groups, due to this their ionization state depends on the pH of the GI compartment and the pK_a value of the compound. In accordance with the physicochemical principle of "like dissolves like", the ionized form exhibits greater aqueous solubility than the neutral form, owing to its enhanced polarity. Fig. 5. illustrates the pH-dependence of solubility of molecules with different acid-base characteristics. Molecules without ionizable functional groups do not show pH-dependent solubility.

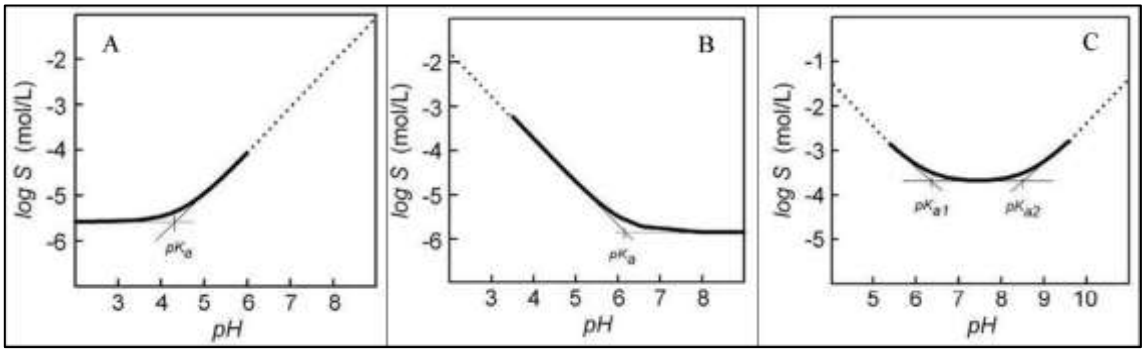

Figure 5. Solubility-pH profile of an acid (A), a base (B) and an amphoteric compound (C) [38]

The thermodynamic solubility of an API can be estimated using the Henderson–Hasselbalch (HH) equation, provided that the pK_a and the intrinsic solubility of the molecule are known.

However, deviations from the predicted curve occur, which can be due to several factors: aggregate or micelle formation, salt effect, or some interaction between the molecule and a buffer component [39–41].

Buffer composition

During solubility measurements various buffers can be used, based on the desired pH. In certain cases, a pH-solubility profile is required, which necessitates a wide pH range of the applied buffer, such as the Britton-Robinson buffer (BRB). In other cases, the measurements are performed at more biorelevant pH values, like in a pH 7.4 phosphate buffer, which simulates the blood. The buffer capacity of these buffers can be different, therefore the solubility of the compound can be affected, so it is important to select a buffer with sufficient capacity near the desired pH.

After *Galia et al.* [42] introduced FaSSIF (fasted-state simulated intestinal fluid) and FeSSIF (fed-state simulated intestinal fluid), which mimic the intestinal conditions before and after a meal, and *Dressman et al.* [43] emphasized the relationship between the pH values and the composition of the two media, the application of biorelevant media became widespread. These contain bile salts like taurocholic acid and phospholipids like lecithin. These components form micelles, thereby improving the solubility of poorly soluble drugs [44,45]. The simulated gastric fluid (SGF) has also been further developed by *Jantratid et al.* [46] to simulate the "early" (0-75 min), the "middle" (75-165 min) and the "late" (after 165 min) phases of postprandial digestion after food intake [47].

Ionic strength, counterion and salt effect

Not only the buffer composition, but the ionic strength also affects the solubility of a molecule. In the case of a neutral molecule or the uncharged form of an ionic compound, higher ionic strength can reduce the solubility of the molecule due to the salting-out effect. On the contrary, lower ionic strength can help dissolve neutral molecules, as it reduces the zeta potential, but not to the extent that it favours hydrophobic interactions [48].

Salts can differ in some physicochemical properties, like solubility, from the free acid or base form. The pH-solubility profile of a salt can be expressed with two independent curves: one where the free acid/base is the saturation species and the other where the salt is the equilibrium species as shown in Fig. 6. The free acid/base and the salt can only coexist as a solid at one point, at the pH_{max} value [49].

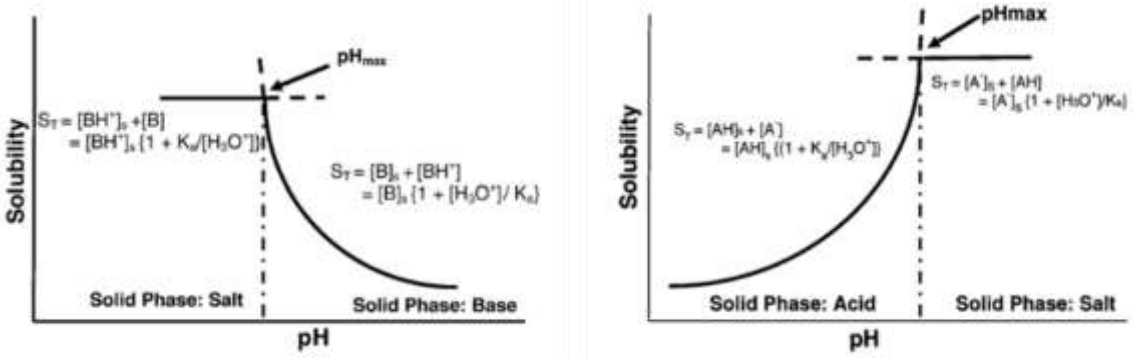

Figure 6. pH-solubility profile of a base (left) and an acid (right) in case of salt formation [49]

Because of the following equilibrium (Equation 1.), in case of salts the increasing level of counterions reduces solubility due to shifting the equilibrium towards the formation of solid salt [48–50].

$$[BH^+X^-]_{solid} \rightleftharpoons [BH^+]_{aq} + [X^-]_{aq} \qquad (1)$$

Particle size

The change in the particle size of the compound affects the solubility and the dissolution as well. The surface area of the APIs increases by reducing particle size, and as a result the dissolution rate improves. The relationship between dissolution and particle size can be described by the modified Noyes-Whitney equation (Equation 2):

$$\frac{\Delta c}{\Delta t} = D*A(\frac{c_s - c_x}{h}) \qquad (2)$$

where $\frac{\Delta c}{\Delta t}$ is the dissolution rate, D is the diffusion coefficient, A is the surface area, h is the thickness of diffusion boundary layer, c_s is the equilibrium solubility and c_x is the concentration in bulk solution at a given time.

According to the equation, the dissolution rate increases with the surface area, but the equilibrium solubility remains unchanged.

However, when particles are reduced to the nanoscale, the Ostwald-Freundlich equation (Equation 3.) indicates that equilibrium solubility becomes dependent on the nanoparticle radius due to the increased surface area [51,52].

$$\log\frac{c_s}{c_\infty} = \frac{2\sigma V}{2{,}303RT\rho r} \quad (3)$$

where c_s is the saturation solubility of the nanonized drug, c_∞ is the saturation solubility of an infinitely large drug crystal, σ is the interfacial tension, V is the molar volume and r is the radius of the molecule.

Crystal form

The solubility of a compound is greatly affected by its crystalline structure. High lattice energy or limited solvation potential can result in low solubility. Additionally, a molecule can crystallise in several polymorphic forms, each with distinct physicochemical characteristics, including solubility. During the dissolution process, these forms may interconvert, or hydrates or solvates may form, which is why analysing both the initial and final solid state is crucial.

Beyond crystalline forms, compounds can also exist in amorphous states, which lack a defined structure, thus without the influence of lattice energy, amorphous materials have higher Gibbs free energy and enhanced solubility. However, this form is thermodynamically unstable and may crystallize in solution. This state can be stabilized by applying various excipients, such as polymers, enhancing solubility [53–55].

Temperature

Dissolution, as a thermodynamic process, occurs spontaneously if the Gibbs free energy change (ΔG) in the system is negative. The Gibbs free energy is influenced by the enthalpy change (ΔH), entropy change (ΔS) and temperature (T) of the system, according to the Gibbs equation (Equation 4):

$$\Delta G = \Delta H - T * \Delta S \quad (4)$$

When a solid dissolves, entropy typically increases because the system becomes more disordered as the particles of the solid separate. Breaking the bonds between solid particles requires energy, this is the lattice energy. If the solvation energy is less than the lattice energy that holds the crystal together, the process is endothermic, and solubility increases with temperature. On the other hand, if the solvation energy exceeds the energy

required to break the lattice, dissolution is exothermic, and solubility decreases as temperature rises. If there's no heat exchange during dissolution, temperature changes do not affect solubility [56].

Based on this, precise temperature control is essential during solubility measurements. Further on, using biorelevant temperatures in the experiments is very important: 32 °C of the skin surface at transdermal delivery and 37 °C of the body for orally applied drugs.

1.3.3. Solubility enhancing methods

As previously mentioned, the majority of novel APIs exhibit low aqueous solubility. This highlights the importance of solubility enhancement during formulation development. Strategies to improve solubility involve physical techniques, such as reducing particle size and forming solid dispersions, as well as chemical strategies, including salt or co-crystal formation. Various excipients – such as surfactants, polymers, and cyclodextrins – are applied during these processes [57–59].

Particle size reduction

Particle size reduction is a commonly used technique for enhancing dissolution and solubility of poorly soluble drugs. Reduction in particle size improves the dissolution rate due to the increased surface area as described in the Noyes-Whitney equation. If nanoscale has been reached, the solubility is directly proportional to particle size (see above the Ostwald-Freundlich equation) [51].

Particle size reduction is done by different techniques like micronization, spray drying, or milling. However, some limitations need to be mentioned, such as the tendency of aggregation, or the degradation of the APIs due to thermal or mechanical stress [57,59,60].

Inclusion-complex formation

CDs are cyclic oligosaccharides and categorized as α, β, or γ CDs based on whether they contain 6, 7, or 8 α-D-glucopyranose units. Their external surface is hydrophilic, while the internal core is hydrophobic. This structure enables them to encapsulate

hydrophobic substances within their internal cavities, leading to the formation of host–guest complexes, significantly enhancing their solubility in water [58,59].

There are various methods for the preparation of inclusion complexes. One of the most commonly used method is spray-drying. In this case, the API is dissolved in a CD solution, and then the solvent is removed. Another option is co-precipitation, where the guest is dissolved in ethanol or other organic solvents and added to the aqueous solution of the CDs. Then it is cooled, and the precipitate can be filtered out [61].

Solubilization by surfactants

Surfactants are widely used solubilizing excipients, characterized by having a polar and a non-polar region. Based on their polar part, surfactants can be ionic or non-ionic. They exert their influence by micelle formation above their critical micelle concentration (CMC). Also, they can lower the surface tension between the compound and the solvent, improve wetting, thus enhancing the solubility of lipophilic drugs in an aqueous environment.

In practice, both non-ionic (e.g. polysorbate) and ionic surfactants – anionic (e.g. sodium lauryl sulfate) and cationic (e.g. cetrimonium bromide) – are commonly applied for this purpose [57,58].

Solid dispersions (SDs)

Nowadays, the formation of solid dispersions is a common form of solubility enhancement. The first generation of SDs were poorly soluble crystalline compounds in crystalline carriers. Recently, instead of crystalline API forms, amorphous ones have been applied. Since the amorphous forms of the APIs are thermodynamically unstable, the amorphous state has a tendency to recrystallize. Polymers, such as polyvinylpyrrolidone (PVP), are commonly used to increase the stability of amorphous solid dispersions. Among the various methods available, spray drying, and hot melt extrusion stand out as the predominant methods employed for SD production within the pharmaceutical field [58,59].

Lipid-based formulations (LBFs)

Lipid-based formulations provide a suitable formulation strategy for enhancing the solubility and oral bioavailability of poorly soluble compounds. LBFs can be classified into four groups based on their composition. Type I LBFs are releasing drugs on digestion, because they cannot be dispersed in aqueous media. Type II contains the self-emulsifying systems, which contain lipids and surfactants with a lower hydrophilic-lipophilic balance (HLB) value than 12. Type III LBFs have HLB values over 12 and contain also hydrophilic cosolvents next to lipids and surfactants, while Type IV formulations are lipid-free systems, consisting only of surfactants and cosolvents. The advantages of LBFs are largely attributed to their ability to stimulate endogenous lipid digestion and lymphatic transport, thereby decreasing first-pass metabolism and improving systemic bioavailability. However, formulation complexity and stability concerns can be a limiting factor of this method [58,62].

1.4. Permeability

According to the Biopharmaceutical Classification System, permeability is the other key factor influencing the bioavailability of a drug in the case of oral administration. Due to this, the investigation of permeability in the early stage of drug development is essential.

Permeability, unlike solubility, is a kinetic physicochemical parameter that determines the rate at which a molecule can penetrate through the membrane (Fig. 7.).

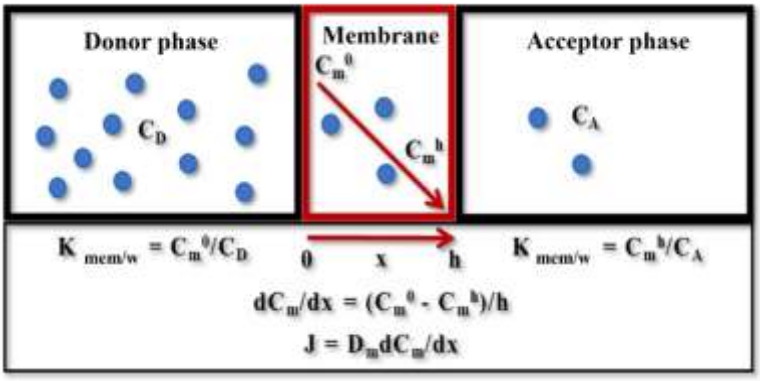

Figure 7. Schematic illustration of the flux. C_D and C_A: the concentration of the permeated molecule on the donor (*D*) and on the acceptor (*A*) side; C_m^0 and C_m^h: the initial and the end concentration in the membrane; *h*: thickness of the membrane; *J*: flux; D_m: diffusion coefficient within the membrane; $K_{mem/w}$: membrane-water partition coefficient [63]

The membrane permeability of a compound can be described with Equation 5.

$$P_m = \frac{D_m \cdot K_{mem/w}}{h} \qquad (5)$$

Assuming that the donor-side concentration is significantly higher than the concentration of the acceptor side, the latter is negligible, thus the flux through the membrane can be expressed using Equation 6,

$$J = P_m \cdot C_D \qquad (6)$$

where J is the flux of the molecule through the membrane, P_m represents the membrane permeability and C_D refers to the drug concentration on the donor side.

Permeability can be described with different constants, depending on how detailed the evaluation of the process is intended to be.

1.4.1. Types of permeability

Apparent permeability (P_{APP})

P_{APP} simplifies the absorption model by neglecting membrane retention, assuming all molecules penetrate through the membrane and reach the acceptor side.

Intrinsic permeability (P_0)

P_0 represents the permeability of the unionized form of a drug. This is significant in the case of ionizable drugs, where the ability to permeate depends on the ionization state of the molecule.

Effective permeability (P_e)

In this model, the membrane is an active participant between the donor and acceptor phases. During the calculation of P_e the membrane retention is taken into account, thereby offering a more accurate *in vivo* prediction for drug absorption.

P_e can be determined by Equation 7 [64]:

$$P_e = -\frac{2.303 V_D}{A \cdot (t - \tau_{LAG})\, \varepsilon_a} \left(\frac{1}{1+r_a}\right) log_{10}\left(-r_a + \left(\frac{1+r_a}{1-R}\right)\frac{c_D(t)}{c_D(0)}\right) \qquad (7)$$

where V_D and V_A is the volume of donor and acceptor compartment (mL), A is the area of membrane, t is incubation time (s), τ_{LAG} is the steady-state time (s), ε_a is the apparent membrane porosity, $C_A\,(t)$ is the concentration of the acceptor compartment after the incubation, $C_D\,(0)$ is the initial concentration of the donor compartment and $C_D\,(t)$ is the concentration of the donor compartment after the incubation. R is the membrane retention factor, calculated by the following equation (Equation 8):

$$R = 1 - \left(\frac{c_D(t)}{c_D(0)} - \frac{V_A}{V_D}\frac{c_A(t)}{c_D(0)}\right) \qquad (8)$$

and r_a is the sink asymmetry ratio (gradient-pH-induced):

$$r_a = \left(\frac{V_D}{V_A}\right)\frac{Pe_{A\to D}}{Pe_{D\to A}} \qquad (9)$$

1.4.2. Factors affecting permeability

GI system and pH

The GI environment significantly affects the permeability of APIs. For ionizable molecules, pH changes between compartments alter the balance of charged and uncharged forms. Passive diffusion primarily favours the neutral form, which predominates for acids in the stomach due to its lower pH, while for bases, in the more alkaline small intestine.

Food can also influence gastric conditions, like modifying the pH, the transit time or the secretion of bile acids.

Covering the entire intestinal epithelium, a mucous layer – composed of water, glycoproteins, electrolytes, proteins, and nucleic acids – plays a key role in drug absorption. This layer forms part of the unstirred water layer (UWL), which can affect the permeability of lipophilic compounds. The rate at which lipophilic molecules penetrate this layer can also act as a limiting factor [10,38,65].

Membrane structure

The cellular membranes can be described as phospholipid bilayers, which are built by charged and uncharged phospholipids, fatty acids, cholesterol, and proteins. They are capable of hydrophobic and hydrophilic interactions. The two most common ways through the membrane are the transcellular and paracellular absorption.

The penetration across the membranes can be influenced by the fluidity and the charge of the membrane, which depends on its composition. In the different compartments of the human body, the biological membranes are varied in the protein:lipid ratio. The higher cholesterol concentration decreases permeability because of its stabilizing function, which increases membrane rigidity. A similar effect can be detected in the case of high phosphatidylcholine concentration. In the case of negatively

charged phospholipids – such as phosphatidylserine – and positively charged drug compounds, ion-pairs can be formed, which can lead a higher permeation [66–68].

The number of tight junctions and efflux transporters in the membrane can also be a limitation factor, like in the case of the blood-brain barrier (BBB) [69].

Molecular size and structure

The permeability of the APIs is influenced by their molecular size and structure. As "Lipinski's rule of 5" describes molecules with a molar mas below 500 Da permeate more easily across the membrane. Also, higher oral bioavailability is found to be associated with lower hydrogen bond counts because, before penetration, these bonds need to be broken. Molecular flexibility and the corresponding ability to undergo conformation changes also play a crucial role in permeability, due to their influencing effect on polar surface area [17,67,70].

1.5. *In vitro* methods for the evaluation of solubility and permeability

1.5.1. Determination of aqueous solubility

Various techniques have been established to measure both thermodynamic and kinetic solubility, using both conventional and HTS methods.

For the determination of kinetic solubility, the first method was turbidimetric measurement introduced by *Lipinski et al*. [17]. Following this, several methods have been developed, such as nephelometry, direct UV, and ultrafiltration LC/MS. These HTS methods are valued for their efficiency – they use small quantities of material, enable testing of multiple compounds simultaneously, and save time. Still, they come with drawbacks, including the possibility that the solid phase formed is not crystalline, pH drift happening during measurements, and concerns about reproducibility [3,19,36].

Several methods are available for measuring thermodynamic solubility, but the „gold standard" is still the saturation shake-flask (SSF) method. Following the work of *Avdeef et al*., potentiometric techniques, such as dissolution template titration (DTT) and the CheqSol method, have been introduced [71–73]. HTS options, including miniaturized shake-flask methods and plate-based assays, have also been established. Moreover, the μDISS Profiler (Pion Inc., Billerica, USA) has been developed as a small-volume

dissolution testing system capable of assessing both kinetic and thermodynamic solubility [3,38,74].

The following sections provide a detailed description of the SSF method and the μDISS device.

1.5.1.1. Saturation shake-flask (SSF) method

SSF is a five-step method that includes sample preparation, reaching equilibrium, phase separation, characterization of the saturated solution and the remaining solid, and then data evaluation [35].

The measurement is performed using an excess of solid under thermostated conditions. After equilibrium is achieved, the phases of suspension have to be separated, preferably by sedimentation, or if necessary, filtration or centrifugation can be applied. Afterwards, the concentration of the solution is detected, most commonly by UV spectroscopy or HPLC, while solid-phase analysis may involve Raman or IR spectroscopy, solid-state NMR, or PXRD [3,38,74].

Due to lack of standardization, earlier studies varied widely in equilibration times (from 48 hours to two weeks) and phase separation techniques. *Baka et al*. published a new, faster protocol by examining the parameters affecting solubility, which can standardize the measurement process. The recommended measurement time is therefore 24 hours, of which 6 hours are for stirring (agitation) and 18 hours for sedimentation [34].

While this method ensures high reproducibility, it is limited by the fact that it is extremely time-consuming. This makes it unsuitable for medium- or high-throughput screening.

1.5.1.2. μDISS

This device consists of small sample chambers (ranging from 2 to 20 mL), into which six stainless steel UV probes are inserted, enabling real-time monitoring of dissolution and solubility. Quantitative analysis requires prior calibration. The early, steep part of the dissolution curve reveals information about the dissolution kinetics, whereas the plateau phase provides the equilibrium solubility value [3,75].

The advantage is that the device can eliminate the interfering effects of solid substances using various mathematical approaches, thereby phase separation is not needed.

1.5.2. Determination of permeability

Various *in vitro* methods have been developed for the investigation of permeability. The most commonly used models are the different *in vitro* cell cultures, like CaCo-2 or MDCK cells, and the *in vitro* Parallel Artificial Membrane Permeability Assay (PAMPA) [76].

Recently, a novel artificial model PermeaPad^{TM} has been developed. It contains a dry phospholipid layer between two cellulose hydrate sheets, after hydration the phospholipids swell and form a bilayer structure similar to cell membranes. Its predictive capacity has been investigated in several studies, which report acceptable *in vitro–in vivo* correlation, with the additional advantage of the absence of organic solvents [77,78].

The following sections provide a detailed description of the *in vitro* cell-based and PAMPA models.

1.5.2.1. *In vitro* cell culture models

The most widely used intestinal cell culture model is CaCo-2, which is isolated from human colorectal carcinoma and has many properties to mimic normal intestinal epithelium. When grown, it forms a polarized cell monolayer with tight-junctions and microvilli. It also expresses several intestinal enzymes, like CYP enzymes, esterases, and various transporters – both influx and efflux – such as P-gp, MDR1, MRP2. Due to these the main advantage of CaCo-2 is its ability to simulate *in vivo* conditions more closely during the study of drug absorption compared to artificial membrane-based models. However, the model has some drawbacks, including increased cost, a long culturing time (<15 days), and due to its sensitivity, only a narrow pH range can be applied [76,79,80].

Another option is the MDCK cell culture, which is derived from dog kidney cells and shows a good correlation with CaCo-2, with a shorter culturing time (2-6 days) [80].

1.5.2.2. Parallel Artificial Membrane Permeability Assay (PAMPA)

Parallel Artificial Membrane Permeability Assay **(**PAMPA) is a 96-well microtiter plate system, with a donor and acceptor compartment separated by a PVDF filter. The artificial membrane is suitable for the determination of passive diffusion, focusing on transcellular transport. The first model was developed by *Kansy et al.,* and the PVDF filter impregnated with egg lecithin dissolved in n-dodecane, served as the membrane [81]. Since then, various techniques have been developed to model different tissues. In BBB-PAMPA porcine brain lipid extract is used for the investigation of permeation through the blood-brain barrier (BBB) [82,83]. Recently, a nasal-PAMPA model has been published, which uses phosphatidylcholine dissolved in n-dodecane as the membrane, and the donor side contains mucin to model mucoadhesion mechanisms [84]. A cornea-PAMPA has been developed as well, using phosphatidylcholine as membrane. The model's applicability was also studied in the case of eye drops, and the results show a good correlation with standard methods [85,86].

The following sections describe gastrointestinal (GIT)- and Skin-PAMPA in detail, because these methods were used during my work.

GIT-PAMPA

The schematic illustration of PAMPA is shown in Fig. 8. The donor side contains the investigated API dissolved in a buffer. The acceptor side represents the blood circulation with a pH 7.4 buffer. The transport effect of blood circulation can be modelled using a sink condition. This is either a single-sink condition, when the pH value of the donor and acceptor compartments is the same (iso-pH condition), but the volume of the acceptor media is bigger compared to the donor side, or it is changed with fresh buffer every sampling time. Another option is the use of chemical scavengers, such as sodium lauryl sulfate (SLS) or hydroxypropyl-β-cyclodextrin (HPβCD), which mimic the presence of serum proteins in blood.

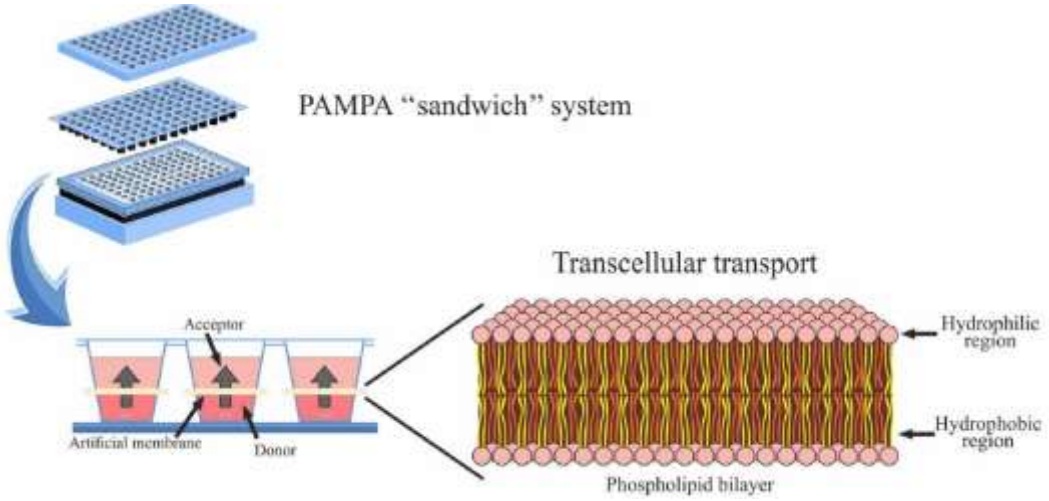

Figure 8. Schematic illustration of PAMPA [87]

The Double-Sink PAMPA (DS-PAMPA) model was established to more accurately simulate *in vivo* physiological environments. DS-PAMPA uses a pH-gradient between the aqueous compartments. The donor side pH can be adjusted to mimic the GI compartment, while the acceptor media is maintained at pH 7.4. To establish the second sink, a micelle-forming or complexing excipient is utilized in the acceptor phase. Further advantage of this model is the introduction of individual well stirring, which enables the UWL to be controlled, leading to a shorter measurement time [3,28,83].

For the better simulation of different tissues, the lipid composition of the membrane was extensively investigated [88].

Skin-PAMPA

The first permeation model for skin was published by *Ottaviani et al.*, although they used silicone oil and isopropyl-myristate as membrane, which are not the natural components of skin [89].

As a result, the focus of further research was to develop a membrane similar to the *stratum corneum*, which mainly consists of ceramides, cholesterol and free fatty acids. *Sinkó et al.* established Skin-PAMPA™, with a membrane created by cholesterol, free fatty acids and certramides [64]. Although synthetic certramides are structurally different from ceramides, their similar molecular mass and hydrogen bond acceptor/donor capacity make them suitable to replace ceramides in the membrane. Skin-PAMPA is a model that offers high reproducibility, it is more cost-effective and less laborious than other *in vitro* skin experiments. The model proved to have high prediction capability with a good

correlation to human skin penetration data. Its applicability has been demonstrated for solute and semi-solid formulations as well as transdermal patches, making it a useful prediction tool for both the pharmaceutical and cosmetic industries [63,90,91].

1.5.2.3. Diffusion cell methods

The diffusion cell is categorized into two main classes: the static (vertical or horizontal) and the flow-through cell. The vertical cells or Franz-cells can be open or closed at the top. In the case of open systems, the measurement is based on the pressure of the air, while for closed devices the pressure is higher, which causes higher permeation values. Fig. 9. illustrates the schematic composition of Franz cell, which contains a fixed volume acceptor chamber with a magnetic stirrer, a donor compartment, a temperature control system, and a port for fluid sampling. As a membrane both animal and human tissue can be used [92,93].

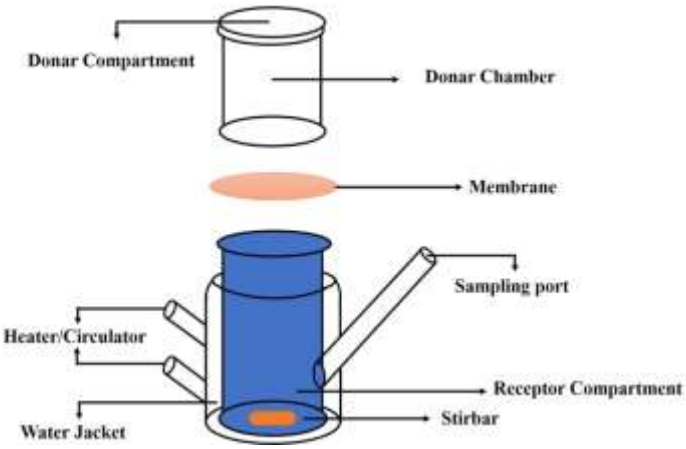

Figure 9. Schematic illustration of Franz-cell [92]

In contrast, the flow-through cells have a steady flow of the receiver medium, which creates turbulence in the acceptor chamber and mimics stirring. Flow-through cells have a receptor chamber with a fixed volume, controlled temperature, and a flexible flow rate [92,93].

1.5.3. *In vitro* simultaneous dissolution-permeation (D-P) tools

Simultaneous dissolution–permeation (D–P) systems are useful tools in the investigation of drug absorption, as they are suitable for modelling both dissolution kinetics and transport across membranes. The aim of these systems is to more accurately

model the gastrointestinal environment and thus provide better *in vivo* prediction. Several D-P systems have been developed, which can be classified by the composition of the membranes (cell free or cell cultures) and geometric setup (horizontal or vertical) [94].

1.5.3.1. µFLUX

One of these systems is the µFLUX technique, which is a suitable tool for the simultaneous investigation of dissolution and permeation. It is a small volume (15-20 mL) apparatus, which consists of two compartments: a donor and an acceptor chamber separated by a PVDF membrane (Fig. 10.). The donor compartment represents the GI system, while the acceptor the blood circulation. It is applicable for evaluating pure APIs and small dosage forms (powder mixtures, mini tablets). Thus, the dissolution of the API from the formulation and its permeation across the membrane can be detected in real time with UV probes. Furthermore, it is a useful tool for the prediction of bioequivalence, as some recent studies have shown in the case of amorph solid dispersions and pH modifiers [95–97].

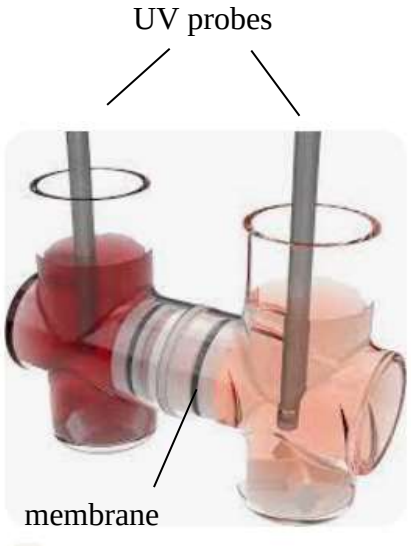

Figure 10. Illustration of µFLUX

1.5.3.2. MacroFLUX

The large-scale device, known as MacroFLUX (850-1000 mL) is a USP 1 or 2 dissolution apparatus combined with a permeation chamber. Its larger volume makes it suitable for the investigation of final dosage form [98].

1.5.3.3. PermeaLoop

PermeaLoop is a novel system for the investigation of simultaneous D-P, consisting of 3 compartments (a donor and acceptor reservoir, a peristaltic pump and a permeation cell), as presented in Fig. 11. The donor and acceptor media are continuously pumped through the looped-shape permeation cells. Although it is a small-scale technique (15-20 mL) its advantage – compared to other methods – is the higher area-to-volume ratio (1.38 cm^{-1}), therefore it is more suitable to mimic the *in vivo* GI situation [94,99].

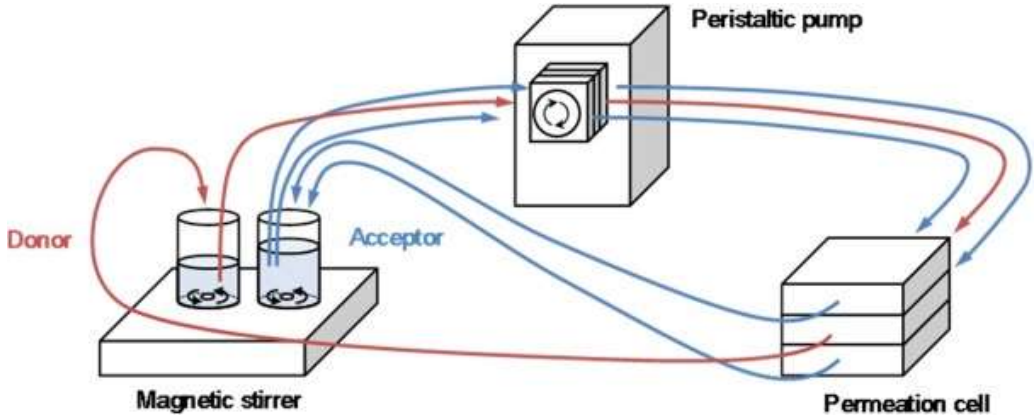

Figure 11. Schematic illustration of PermeaLoop [99]

1.6. Solubility-permeability interplay

As mentioned above solubility and permeability are the two key parameters during the investigation of *in vitro* dissolution and permeation and *in vivo* bioavailability of a drug. Because most novel APIs can be categorized as BCS II or IV compounds, various solubility enhancement methods have been developed. One option is the application of different pharmaceutical excipients during the formulation process. While the effect of the excipients was extensively investigated on solubility, their influence on permeability was neglected, until *Dahan and Miller's* pioneering work. Through various studies an inverse relationship between solubility and permeability has been demonstrated [100–102].

Surfactants

Surfactants are one of the most commonly used excipients, due to their ability to increase solubility tremendously via micelle formation. They can be ionic or non-ionic

amphiphilic molecules with a polar head and apolar chain. Although their solubilizing effect is obvious and useful, the concurrent reduction in the free fraction of the molecule leads to lower permeability, due to the decreased drug concentration gradient [101,102].

As was reported, the effect of surfactants on permeability can be more complex due to their ability to solubilize intestinal epithelial cells, leading to the damage of the intestinal barrier, resulting in increased paracellular transport [103].

Cyclodextrins

As previously mentioned, CDs have a cyclic structure with a hydrophilic external surface and a hydrophobic inner cavity, which allows them to encapsulate a lipophilic molecule inside the cavity. The inclusion complex formation significantly improves the apparent solubility of the drug. Similarly to surfactants, their solubility-permeability trade-off can be complex [104].

On one hand, CDs can reduce permeability by lowering the concentration of the free fraction of the APIs [104,105]. Yet, in contrast, some studies have shown enhanced permeability in the presence of CDs. This may be the result of their ability to interact with membrane cholesterol, which causes a change in membrane fluidity and leads to a higher permeability value [106]. Furthermore, when drug transport is limited by the UWL, CDs can improve transport across the membrane by facilitating faster diffusion through the UWL [107].

Cosolvents

Cosolvents (e.g. propylene glycol, polyethylene glycols, dimethyl sulfoxide) are less polar than water, due to this they decrease the polarity of the GI system, which leads to a smaller difference in polarity between the drug and its environment. Their hydrogen-bonding groups enhance the drug's solubility in water, while the hydrophobic parts of their structure disrupt the hydrogen bond network of water.

Cosolvents, in contrast to cyclodextrins and surfactants, do not affect the concentration of the free fraction, yet still cause a decrease in permeability. This phenomenon can be attributed to the relationship between drug permeability (P) and membrane/water partition coefficient (K). Increased cosolvent concentrations raise the

apparent solubility of the drug but reduce the membrane/water partition coefficient, ultimately diminishing permeability [108,109].

Polymers

Polymers have been widely used in the pharmaceutical industry, due to their diverse physicochemical properties they can be utilized for different purposes, like stabilizers, binders, and solubilizing agents. Based on these, their effect on permeability is not so obvious. While some polymers influence intestinal permeability, others show minimal or no effect, depending on the ability to form various hydrophilic and hydrophobic interactions [104].

Hydrotropes

Like surfactants, hydrotropes contain a hydrocarbon fragment and an ionic part, due to this they have moderate surface activity. However, unlike surfactants, hydrotropes' HLB values are higher due to their shorter alkylchain tail. As a result, significantly higher concentrations of hydrotropes are needed to enhance the solubility of hydrophobic compounds. Hydrotropes can increase solubility via several mechanisms, such as self-aggregation, depression of water activity, and interactions between the drug and the amphiphilic excipient, although they don't have the ability to form micelles [104,110].

For the investigation of solubility-permeability interplay, the effect of two commonly used hydrotropes (urea and nicotinamide) was studied in the case of carbamazepine. Both hydrotropes enhanced the solubility of carbamazepine in a concentration-dependent way, while both *in vitro* and *in vivo* permeability decreased [111].

This highlights the importance of simultaneously evaluating both parameters when developing solubility-enhancing formulations.

2. Objectives

The aim of my research work was to investigate two physicochemical parameters – thermodynamic solubility and permeability – in the presence of various formulation excipients in the case of oral and transdermal administration. The study focused on these two drug delivery routes since oral administration is the most prevalent route, while transdermal systems are garnering greater research interest due to improvements in the cosmetic sector. Additionally, I aimed to perform a comprehensive analysis to elucidate the relationship between the two examined physicochemical parameters under different conditions, hence aiding in the formulation development.

- Study of the impact of different solvents on transdermal permeability
  - Investigation of the HT Skin-PAMPA method to demonstrate its applicability as a screening tool in the case of apolar molecules and different solvents. Phenylethyl resorcinol, a skin-lightening agent, was chosen as a model compound, and 13 solvents and mixtures of solvents with different polarity, commonly used in the cosmetic industry, were applied.
  - Development of a simple method for assessing membrane integrity, essential for PAMPA measurements, as it ensures that the model accurately simulates passive diffusion across artificial membranes. Monitoring membrane integrity is essential for reproducibility and accurate correlation with *in vivo* absorption data.
  - *Ex vivo* permeability assessment of the model compound on porcine ear skin utilizing the Franz-cell method to acquire data for comparison with PAMPA results. Identification of the optimal permeability parameters to establish the most accurate correlation with the animal skin model.
- Study of the effect of excipients on solubility and GI permeability and their interplay
  - Investigation of the effects of nine pharmaceutical excipients – used in oral formulations – on the thermodynamic solubility and intestinal permeability of three model compounds: carbamazepine, naproxen, and pimobendan.
  - Executing a comprehensive investigation to examine the effect of excipients as a function of pH, their concentration, and the acid-base character of the model compounds.

- Based on our measurements, it can be observed that the examined excipients can influence the solubility and permeability various ways. Consequently, certain correlations can be established between these two parameters, thus enabling the optimal excipient selection.

3. Materials and Methods

3.1. Model compounds

Phenylethyl resorcinol (PER)

Phenylethyl resorcinol (Fig. 12.) can inhibit melatonin synthesis by blocking tyrosinase activity, therefore, it is used in cosmetic industry as a skin lightening agent. It is a non-polar, weak acid (pK_{a1} 9.77; pK_{a2} 10.77), which is neutral at physiological pH, with suitable lipophilicity (log$P$ 2.98) for transdermal delivery [112,113]. PER was obtained from Symrise^{TM} (Holzminden, Germany).

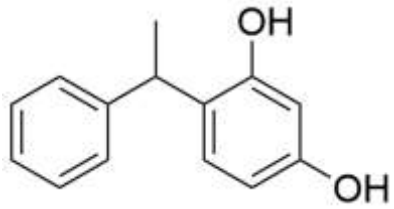

Figure 12. Structure of phenylethyl resorcinol

Carbamazepine (CAR)

Carbamazepine (Fig. 13.) is a BCS Class II drug, used for the treatment of seizure disorders and neuropathic pain. It is a voltage-gated sodium channel inhibitor. CAR is a neutral molecule due to its carboxamide group [114]. CAR was purchased from Sigma-Aldrich Co. Llc. (St. Louis, MO, USA).

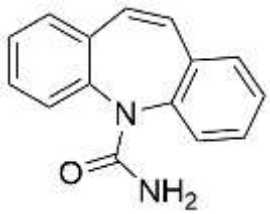

Figure 13. Structure of carbamazepine

Naproxen (NAP)

Naproxen (Fig. 14.) is a nonsteroidal anti-inflammatory drug (NSAID). NAP exerts its effect through the inhibition of cyclooxygenase (COX) enzyme. NAP is a lipophilic weak acid (pK_a 4.14) and as a BCS Class II compound has a low aqueous solubility,

although its solubility and permeability are pH-dependent [19,114]. NAP was purchased from Sigma-Aldrich Co. Llc. (St. Louis, MO, USA).

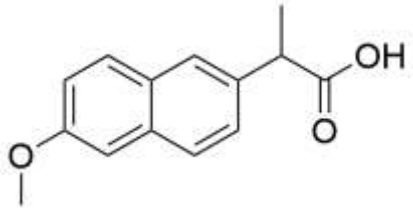

Figure 14. Structure of naproxen

Pimobendan (PIMO)

Pimobendan (Fig. 15.) is a BCS Class II drug, an inodilator that exerts its effect by calcium sensitization and inhibition of phosphodiesterase 3 (PDE3), approved by the US Food and Drug Administration (FDA) for the treatment of heart failure in dogs. PIMO is a weak base (pK_a 4.30) due to its benzimidazole ring, with pH-dependent solubility and permeability [97,115]. PIMO was obtained from Sigma-Aldrich Co. Llc. (St. Louis, MO, USA).

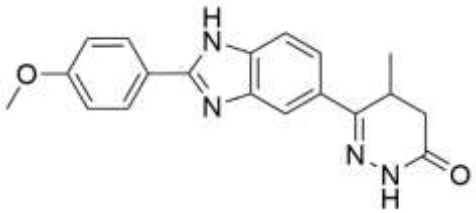

Figure 15. Structure of pimobendan

3.2. Excipients and other materials

All solvents (ethanol, glycerol, dimethyl isosorbide, propylene glycol, capric/caprylic triglycerides, octyl dodecanol, apricot kernel oil and corn oil) for Skin-PAMPA measurements were provided by the French L'Oréal Laboratories. Lucinol used as internal standard for LC/MS-MS PER quantification was received from L'Oreal. Pig ear skin was obtained from a slaughterhouse (Pouldreuzic, France), frozen at -20 °C after sampling and stored prior to use. Piroxicam as a model compound for membrane integrity test was purchased from Sigma-Aldrich Co. Llc. (St. Louis, MO, USA).

For the investigation of solubility-permeability interplay lactose-monohydrate, sorbitol, mannitol, SLS, polyvinylpyrrolidone/vinyl acetate 64 (PVPVA 64),

polyvinylpyrrolidone K25 (PVP-K25), and Polysorbate 80 (Tween 80) were received from Sigma-Aldrich Co. Llc. (St. Louis, MO, USA), HPβCD with the degree of substitution ~4.5 and sulfobutyl-ether-β-cyclodextrin (SBEβCD) with the degree of substitution ~7 from Cyclolab R&D Ltd. (Budapest, Hungary). The buffer components (acetic acid (99-100%), phosphoric acid (>85%), boric acid, sodium hydroxide) were supplied by Molar Chemicals Ltd. (Halásztelek, Hungary). HEPES (2-[4-(2-hydroxyethyl)-1-piperazinyl] ethanesulfonic acid) was purchased from TCI Chemicals (Tokyo, Japan). GIT lipid was received from Pion Inc. (Billerica, MA, USA).

3.3. Methods

3.3.1. Skin-PAMPA membrane integrity test

Possible disruption by solvents of the integrity of the biomimetic artificial membrane was investigated. The Skin-PAMPA plate was hydrated overnight. Then, the wells were filled with each solvent and incubated for at least 7 hours. The solvents were removed from the wells, and a standard measurement was performed using piroxicam as a reference compound, because its permeability data has been investigated previously [63]. The permeability coefficient ($\log P_m$) values were compared with the reference value of untreated plates.

3.3.2. Skin-PAMPA measurements

Membrane permeability of PER was measured using Skin-PAMPA plates (Skin-PAMPA™, Pion Inc., Billerica, MA, USA). Membranes were hydrated overnight with standard hydration solution (Pion Inc™). The donor phase solutions of PER in different solvents were prepared freshly based on the approximate solubility, and 70 µL was applied to the donor (upper) plate. The acceptor (lower) plate contained 180 µL Prisma buffer pH 7.4. The PAMPA™ sandwich was incubated at 32 °C in a Gut-Box™ (Pion Inc™). Stirring bars were applied in both donor and acceptor wells to avoid the effect of the unstirred water layer. Samples were taken after 7.5, 15, 30, 60, 120, 240 and 360 min of incubation, then replaced with fresh buffer solution. 150 µL from the acceptor compartment was transferred to UV plates (Greiner Group AG, Kremsmünster, Austria),

then the absorption was measured at λ = 280 nm with Tecan Infinite M200 UV-plate reader (Tecan™, Männedorf, Switzerland).

3.3.3. Penetration kinetics across pig ear skin

Before use, hairs were shaved from the pig ear skin, and the skin thickness was adjusted to between 700 and 1200 μm. The integrity of the skin was tested according to the Trans-Epidermal Water Loss (TEWL) method using a Delfin device.

During the topical application, PER was applied in an infinite dose (1.13 mL/cm^2), which means that the compound is in large excess in the donor compartment compared to what can permeate through the membrane, to ensure that the concentration gradient is not changed over time [116]. The measurement lasted for 16 h and 200 μL samples were taken every hour, which were replaced with fresh receptor fluid (9 g/L sodium chloride solution with 0.25% Tween 80).

The samples were directly injected into an LC/MS-MS system (Shimadzu Nexera LC system, Shimadzu, Kyoto, Japan) coupled with a mass spectrometer API 3500 (Sciex, Framingham, MA, USA). The analytical column used was a Kinetex C18 from Phenomenex™ (50 x 2.0 mm, d_P 2.6 μm) (Torrance, CA, USA), and the analysis was carried out with gradient elution with mobile phases of 20 mM ammonium acetate (A) and acetonitrile (B) at 50 °C. The volume of the injection was 10 μL with a flow rate of 0.8 mL/min. The ionisation mode used was electrospray negative.

3.3.4. Determination of approximate and equilibrium solubility of PER

As a first step, the solubility class at 32 °C was determined according to the OECD test guideline No. 105 [117]. For this, 0.1 g of the PER sample was precisely weighted in a 10 mL glass-stoppered measuring cylinder. Increasing volumes of solvent were added stepwise, then the mixture was shaken for 10 min and evaluated visually for any undissolved particles. If the sample remained undissolved after addition of 10 mL of solvent, the experiment was continued in a 100 mL cylinder. The approximate solubility is given as the volume of the solvent in which complete dissolution was observed after 1 h. The samples were then stirred for 24 h before a final visual assessment. Based on this method, five solubility categories were set between 1 and 1000 mg/mL.

For solvents tested on pig skin, the solutions were prepared with the concentration set to the upper limit of the solubility class previously defined and they were centrifuged at 14000 rpm to guarantee particle precipitation before analysis. For the determination of concentration, the previously described LC/MS/MS method was used.

3.3.5. Analysis of Skin-PAMPA and pig ear data

In the case of Skin-PAMPA the flux (*J*) was obtained as the slope of the permeability profile during the incubation period between 0 to 30 min, based on the linear regression.

The area under the curve (*AUC*) was calculated by integration of the permeability profile between 0 and 6 h using OriginPro v.2019b (OriginLab Corporation, Northampton, MA, USA).

In the case of pig ear skin measurements, the penetration parameters (permeability coefficient, K_p, and flux) were determined from the curves representing the cumulative amount per unit area of skin (Qt, μg/cm^2) as a function of time (h) based on Equation 10 [19,118].

$$K_p = \frac{Q_t}{h*A} \qquad (10)$$

The calculation was carried out using GraphPad PrismT v.7 (GraphPad Software Inc., San Diego, CA, USA).

3.3.6. Thermodynamic solubility measurements

Thermodynamic solubility was determined in Britton-Robinson buffer (BRB) at 3 different biorelevant pH values (pH 3.0, pH 5.0, and pH 6.5) at 37 ± 0.5 °C by the SSF method. Physical mixtures of excipients and APIs were prepared at 0.5:1, 1:1, and 3:1 mass ratios. In the presence of excess solid, the samples were stirred at 200 rpm for 6 hours; after the first hour, the pH was checked and adjusted as necessary, then it was sedimented for 18 hours [34,35]. At the end of each measurement, the pH was checked again. In cases of incomplete phase separation, filtration (Millex GV 0.22 μm, Ø: 3.3 cm, hydrophilic PVDF membrane) was used [119]. Following calibration, the μDISS Profiler™ (Pion Inc., Billerica MA, USA) equipped with UV probes was used for *in situ* concentration measurement. The 2nd derivative method in AuPRO™ 7.1 was used for concentration determination.

3.3.7. GIT-PAMPA measurements

Each well of the top (acceptor) compartment of a 96-well STIRWELL™ PAMPA sandwich (Pion Inc.) was coated with 4 μL of GIT lipid (Pion Inc.) The acceptor compartment of the plate was filled with 200 μL of pH 7.4 HEPES buffer containing 1% of SLS to maintain sink condition. The donor (bottom) plate was prefilled with 180 μL of the appropriate sample solutions. After assembling the sandwich, it was incubated at 37 ± 0.5 °C. The thickness of UWL in both compartments was set to 60 μm by stirring in Gutbox™ (Pion Inc.). The duration of the incubation depended on the permeability of molecules. Subsequently, 150 μL from both the donor and acceptor compartments were transferred to UV plates (Greiner Group AG). UV absorption (λ=230-400 nm) was measured using Tecan Infinite M200 UV plate reader (TecanTM). P_e values were calculated using the PAMPA Explorer software™ (Pion Inc.).

3.3.8. Analysis of solubility and permeability data

Equilibrium solubility measurements were carried out with three parallel experiments. The determination of P_e was performed in duplicate (there were three parallels within a plate). The permeability and solubility values were compared in each study by analysis of variance using a general linear model and contrast comparison. In the general linear model, the independent variables were the types of excipients at the various mass ratios, while the dependent variables were either permeability or solubility. The analysis was performed separately for each pH condition. As post-hoc analysis general linear hypothesis tests (Dunnett) for multiple comparisons with contrasts were performed. The statistical analysis was performed using the R programming language in R version 4.0.5 (R Foundation for Statistical Computing, Vienna, Austria) [120] and the R Studio integrated development environment (Posit, Boston, MA, USA). The multiple comparisons were performed using the 'multcomp' package [121].

3.3.9. Analysis of particle size

The mean particle size and size distribution of the original compound were determined by Laser Diffractometry.

For Laser Diffractometry, 0.1 mL of milled suspensions were dispersed in 100 mL of demineralized water at a mixing speed of 1500 rpm with Mastersizer Hydro 2000 SM small volume dispersion unit. The particle size of the samples was measured at 25 ± 1 °C using a Mastersizer 2000 (Malvern Instruments Ltd., Malvern, UK). Every sample was measured three times individually, and each measurement took 10 s to perform, suggested by the Malvern diffraction application to allow slow-moving larger aggregates to pass through the detector array.

4. Results

4.1. Investigation of the impact of different solvents on transdermal permeability

As the literature review shows, the usage of the PAMPA model, and within this Skin-PAMPA, has been growing in drug research. However, its applicability when API is dissolved in a wide range of polar and non-polar solvents has not been investigated. Therefore, in the first part of my dissertation work, we studied the effect of different solvents commonly used in the cosmetic industry (Table 1) on the transdermal permeability of model compound phenylethyl resorcinol (PER) by the Skin-PAMPA method. Our primary goal was to prove the usefulness of this HT, *in vitro* technique for the selection of appropriate solvent in the early stage of product formulation.

Prior to the investigation of PER, a simple membrane integrity test had to be developed to ensure that the applied solvents do not damage the artificial membrane.

4.1.1. Membrane integrity test

The visual appearance of the membrane after 7 h pre-treatment with the solvents was checked before the piroxicam aqueous solution was added. The logarithm of membrane permeability ($\log P_m$) values of piroxicam measured across the solvent-treated membranes were in the range of -3.82 and -4.81, with a mean of -4.25±0.30. These findings are in good correlation with the reference value of -4.98±0.01, which was measured previously using the same PAMPA method [63]. The standard deviation (SD) of the permeability values of piroxicam serves as an indicator of membrane integrity. An extremely high SD would indicate membrane damage. As illustrated in Fig. 16., the highest variation – namely ±0.23 – is observed for ethanol (S2), which is still acceptable, indicating an interaction with the membrane rather than its disruption.

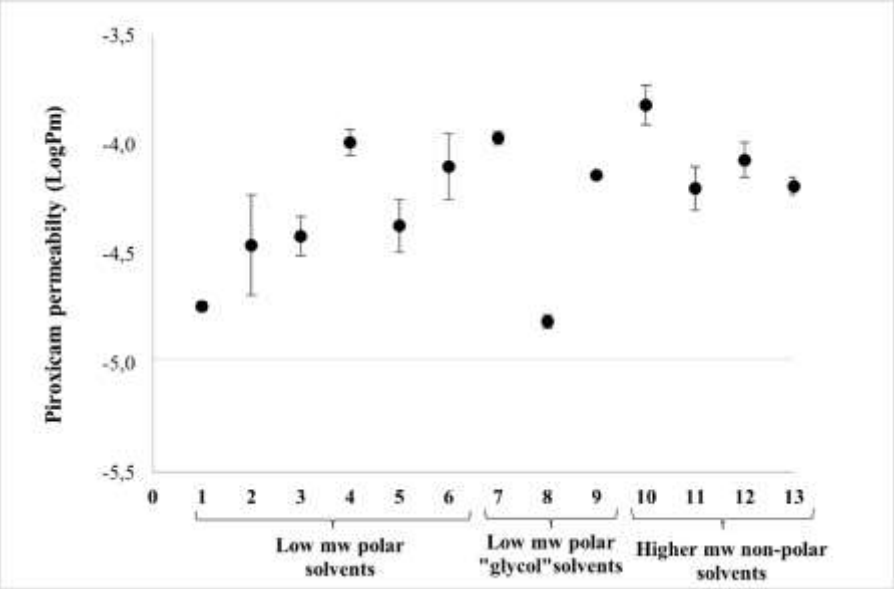

Figure 16. Effect of 13 solvents on the integrity of the Skin-PAMPA membrane using piroxicam as the model compound. The permeability values are mean ± SD, *n*=9.

4.1.2. Skin-PAMPA permeability measurements

During the measurements, phenylethyl resorcinol (PER) was applied as infinite dose. For the application of adequate concentration during the permeability measurements, the solubility of PER was previously determined by a LC/MS/MS method. The solubility results are shown in Table 1.

Table 1. Solvents used in the study and the solubility of PER in different solvents (n.m. - not measured, n.a. - not available)

Solvent class	Code	Solvent	MW of solvent	PER Approximate solubility (mg/mL)	PER Equilibrium solubility (mg/mL)
Low-MW polar solvents	S1	Water	18.0	1	1.3 ± 0.2
	S2	Ethanol	46.1	>1000	368 ± 52
	S3	Glycerol	92.1	5	n.m.
	S4	Dimethyl isosorbide	174.2	75	60 ± 5.7
	S5	Water:ethanol – 80:20 (w/w)	n.a.	10	8.1 ± 4.3
	S6	Water:dimethyl isosorbide – 90:10 (w/w)	n.a.	1	1.08 ± 0.07
Low-MW polar "glycol"solvents	S7	Propylene glycol	76.1	500	350 ± 21
	S8	Water:propylene glycol – 80:20 (w/w)	n.a.	10	5.1 ± 0.8
	S9	Water:propylene glycol:ethanol – 10:30:60 (w/w/w)	n.a.	>1000	373 ± 49
High-MW non-polar solvents	S10	Capric/caprylic triglyceride	554.8/470.7	75	74 ± 5.1
	S11	Octyl dodecanol	298.6	1	n.m.
	S12	Apricot kernel oil	n.a.	1	n.m.
	S13	Corn oil	n.a.	1	n.m.

To obtain relevant information about the effect of the solvent on transdermal permeation, the most characteristic parameters (*J*, lag time, permeated amount, *AUC*, logP_m) were determined from the permeated amount vs. time plot. In the case of infinite dosing, the permeated amount vs. time plot is expected to be linear until the acceptor concentration reaches the limitation of the solubility or the donor side no longer provides the infinite dose. To avoid the limitations, the first 3 timepoints (7.5 min, 15 min, 30 min) were used for the linear regression. The slope of the curve gives the flux (*J*) and the x value when y is 0 the lag time. The calculated lag times (0–6 min) indicated fast membrane saturation of PER regardless of the solvent. The area under the curve (*AUC*) and the permeated amount was calculated from the saturation curves. The donor concentration (C_D) was determined based on the results of solubility measurements. Fig. 17. represents the permeability profile and the linear regression curve – as an example – in the case of water:ethanol (80:20 w/w) mixture. Similar graphs were obtained for all solvents.

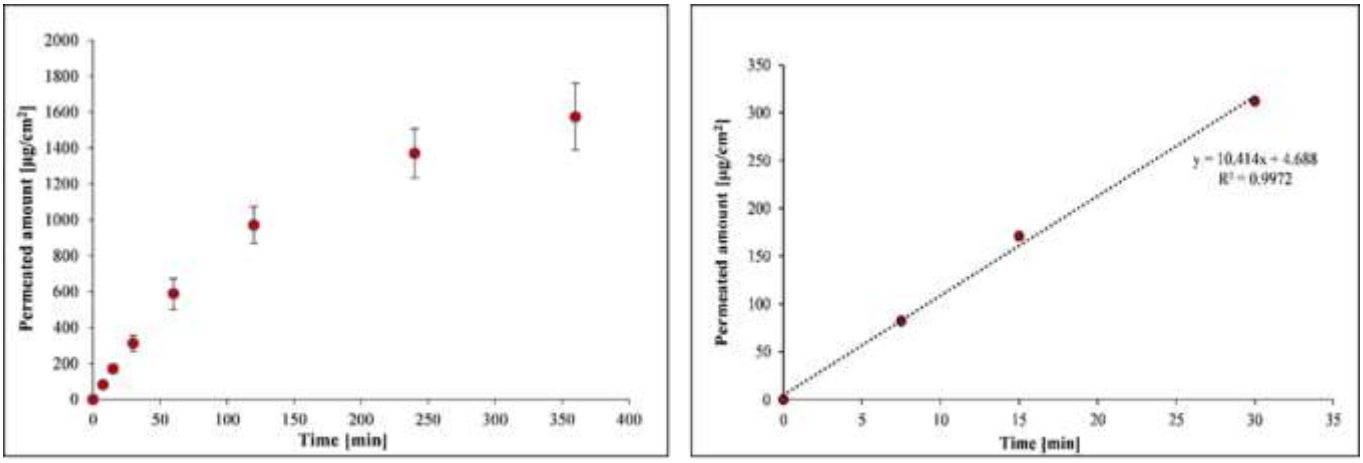

(a) (b)

Figure 17. (a) Permeability profile of PER dissolved in water:ethanol (80:20 w/w) mixture; (b) Linear regression curve of PER in the same solvent mixture.

The studied permeability parameters across the Skin-PAMPA membrane of PER dissolved in different solvents are shown in Table 2.

Table 2. Characteristic parameters of permeability of PER using Skin-PAMPA

Code	C_D [mg/mL]	J [µg/cm²*h]	Lag time [min]	Permeated Amount (6 h) [µg/cm²]	AUC Normalized to C_D [µg/cm²]	logP_m
S1	1	72.38 ± 7.83	1.4	169.2 ± 4.48	647.1	-1.12 ± 0.06
S2	500	12033 ± 252.0	0.0	13575 ± 1710	104.6	-1.62 ± 0.01
S3	5	137.4 ± 21.64	5.5	869.2 ± 112.5	491.3	-1.57 ± 0.07
S4	70	208.6 ± 53.00	3.6	1342 ± 298.2	55.2	-2.54 ± 0.13
S5	10	589.2 ± 25.21	0.9	1662 ± 168.7	568.5	-1.23 ± 0.03
S6	1	76.41 ± 15.20	0.0	174.6 ± 21.69	550.7	-1.13 ± 0.07
S7	500	2118 ± 501.8	3.8	11142 ± 729.6	69.1	-2.38 ± 0.11
S8	10	569.7 ± 4.82	1.1	1772 ± 98.08	595.2	-1.24 ± 0.01
S9	500	10846 ± 326.7	1.4	14926 ± 2431	114.1	-1.66 ± 0.01
S10	70	376.6 ± 33.58	3.0	748.9 ± 91.94	38.2	-2.27 ± 0.04
S11	1	7.18 ± 1.60	3.9	18.91 ± 0.40	64.5	-2.16 ± 0.08
S12	1	2.45 ± 0.57	3.3	13.42 ± 1.90	36.7	-2.63 ± 0.07
S13	1	3.26 ± 0.41	1.4	12.93 ± 1.30	38.6	-2.48 ± 0.06

The permeability of the molecule is greatly affected by the applied solvent. The logP_m value, which was used for the comparison, varied by about 1.5 orders of magnitude. Based on it, the applied solvents can be categorized into three groups.

The first group with *high* permeability (logP_m > -1.25), includes water (S1), which resulted in the highest logP_m value (-1.12± 0.06), and mostly water-containing mixtures

(S5, S6, S8). At the same time, the PER has limited solubility in these solvents (1-10 mg/mL).

The second group resulted in *medium* permeability (logP_m range is -1.5 and -2.3) and its solvents can be divided into two main categories (a) higher-MW non-polar solvents such as long-chain fatty acid esters (S10) and long-chain alcohol (S11), and (b) the small polar alcohols (S2, S3) and a solvent mixture containing glycol and ethanol (S9).

The last group resulted in low permeability (logP_m < -2.4), it contains two main types of solvents as well: (a) low-MW polar organic solvents dimethyl isosorbide (S4) and propylene glycol (S7), where the solubility of PER is high (75 and 500 mg/mL), and (b) higher-MW non-polar solvents in which PER was poorly soluble (~1 mg/mL), namely, apricot kernel oil (S12) and corn oil (S13).

4.1.3. Permeation kinetics across pig ear skin

The permeability of PER was determined for nine solvents, including mostly low-MW polar ones, low-MW polar "glycols", and a non-polar solvent (see data in Table 3.) across pig ear skin by the Franz-cell method. Data were compared with Skin-PAMPA results.

Table 3. Characteristic parameters of permeability of PER across pig ear skin

Code	C_D [mg/mL^1]	J [µg/cm^2*h]	Permeated Amount (16 h) [µg/cm^2]	logK_p
S1	1	25 ± 9.6	261 ± 100	-1.71 ± 0.32
S2	368	20 ± 15	98 ± 67	-4.26 ± 0.51
S4	60	0.08 ± 0.024	1.09 ± 0.39	-5.88 ± 0.19
S5	8	61 ± 18	515 ± 203	-1.97 ± 0.34
S6	1	7.5 ± 3	100 ± 37	-2.16 ± 0.26
S7	350	20 ± 17.6	147 ± 120	-4.24 ± 0.81
S8	51	98 ± 50	516 ± 109	-1.72 ± 0.34
S9	373	40 ± 15	320 ± 149	-3.97 ± 0.24
S10	75	8 ± 3.5	54 ± 34	-3.97 ± 0.29

Fig. 18. shows the correlation curves of the different parameters between Skin-PAMPA and pig ear skin permeability results. In the case of flux (J), the absolute values were higher using Skin-PAMPA than for pig skin. In four solvents (S1, S5, S6, and S8),

the difference was within one order of magnitude, whereas for S4, the flux was overestimated by Skin-PAMPA by two orders of magnitude. However, there were four outliers: solvent S2, S7, S9 and S10, where the difference was more than 3 orders of magnitude.

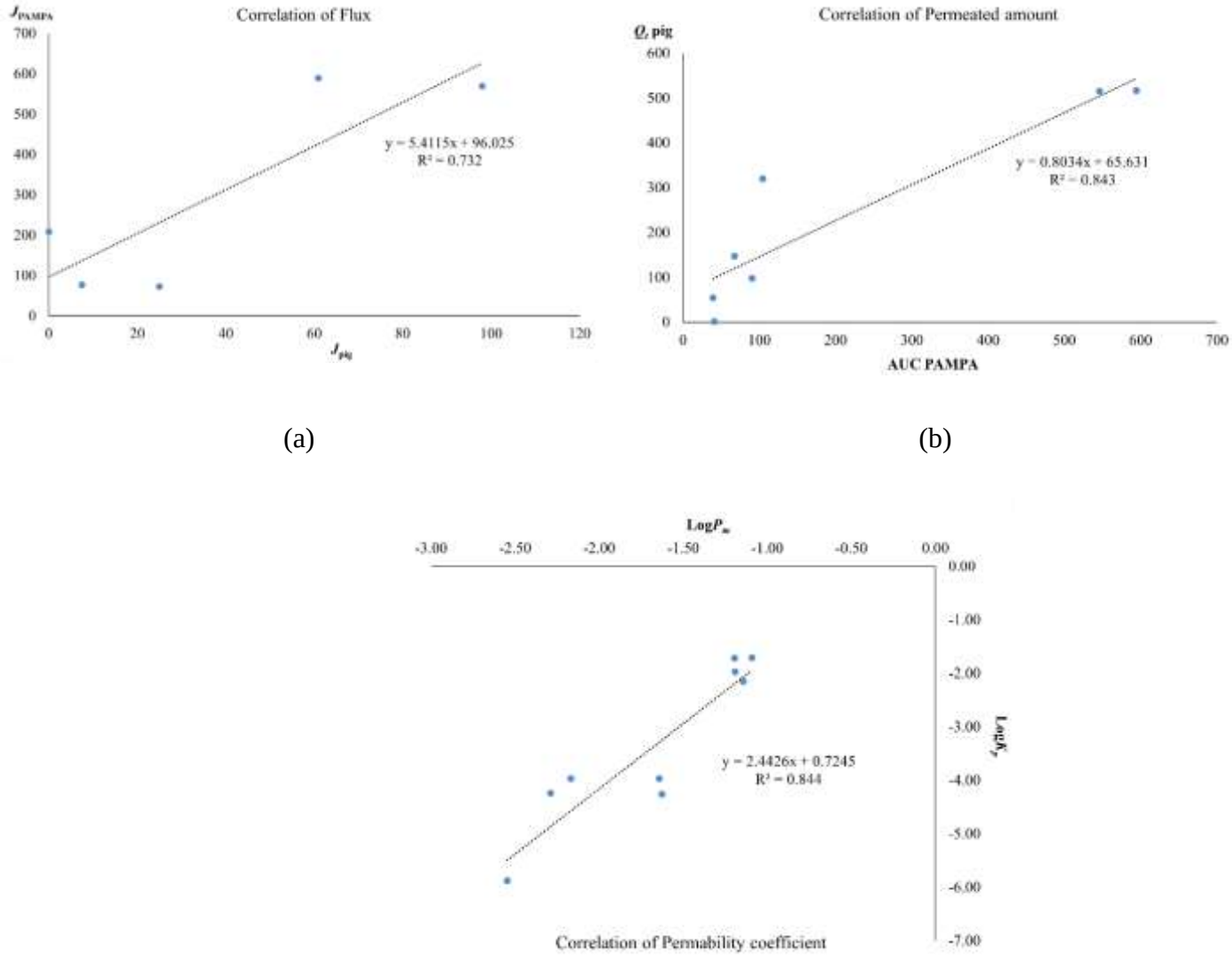

(a) (b)

(c)

Figure 18. Correlation between Skin-PAMPA and pig ear skin permeability results. (a) Correlation curve of flux (no close correlation); (b) Correlation curve of permeated amount (R^2 = 0.843, n = 7); (c) Correlation curve of permeability coefficient, logP_m and logK_p (R^2 = 0.844, n = 9).

The permeated amount was calculated as the integration of the permeability profile, expressed as the AUC_{PAMPA} for Skin-PAMPA and $Qt_{pig\ skin}$ for pig ear skin, and normalized to the donor concentration. These two parameters show a closer correlation (the

correlation coefficient is R^2=0.843) than the flux, yet there were two outliers (S1 and S6) in this case as well.

The best correlation between the two models was obtained when the logP_m for PAMPA and the logarithm of permeability coefficient (logK_p) for pig skin were used. These logP_m values were normalized to the donor concentration, like the permeated amount. However, just as for the flux, the permeability coefficients were higher in the case of the Skin-PAMPA. This phenomenon is expectable when we compare a single membrane with a multiple layered native pig skin. The biggest differences were observed when the PER was dissolved in dimethyl isosorbide (S4) and ethanol (S2). Nevertheless, there was a good correlation between the two values for the nine solvents, with an R^2 of 0.844 without any outliers.

4.2. Study of the effect of pharmaceutical excipients on solubility and GI permeability and their interplay

The literature highlights the fundamental role of solubility-permeability interplay caused by formulation excipients, but so far, mostly only individual drug-excipient interactions were investigated instead of a holistic study. Therefore, in the second part of my research, we studied the influence of formulation excipients – commonly used in oral products – on solubility and GI permeability of APIs with different acid-base character. In the next chapter, the solubility results are summarized first.

4.2.1. Effect of pharmaceutical excipients on solubility

The equilibrium solubility value of the model compounds: CAR, NAP and PIMO was measured by the validated SSF method, in the absence (used as a reference) and in the presence of 9 pharmaceutical excipients at 3 different mass ratios (0.5:1; 1:1; 3:1 – excipient : API). During the selection of excipients, the aim was to identify the most widely used categories of excipients, with emphasis on those frequently utilized in solubility enhancement studies and marketed formulations. Usually, two representatives from each category were chosen. The final selection included sugars and sugar alcohols mannitol and sorbitol, both possessing hydrotropic properties, as well as lactose, a completely inert filler. Cyclodextrins were represented by hydroxypropyl-β-cyclodextrin (HPβCD) and sulfobutyl-ether-β-cyclodextrin (SBEβCD), due to their ability to form

inclusion complexes. Among surfactants, the non-ionic Tween 80 (Polysorbate 80) and the anionic sodium lauryl sulfate (SLS) were selected due to their amphiphilic nature and their frequent application in solubilization. Finally, polyvinylpyrrolidone K25 (PVP-K25) and polyvinylpyrrolidone/vinyl acetate 64 (PVPVA 64) were chosen to represent polymers due to their established role as solubility and stability enhancers. Three biorelevant pH values were applied (pH 3.0; 5.0, and 6.5) for the study of the role of ionization state. The particle size distribution was determined by laser diffractometry to reveal whether there is any effect of the different excipients on this parameter. The particle size data of the APIs are shown in Table 4, using the d10, d50 and d90 values. These values represent the upper size limit in μm below which 10%, 50% and 90% of the particles fall, respectively. Based on it, all the compounds are in the microcrystalline range [122].

Table 4. Particle size distribution of the APIs (d10: 10% of the total particles smaller than this size, d50: 50% of the total particles smaller than this size, d90: 90% of the total particles smaller than this size)

	Particle size (μm)								
	pH 3.0			pH 5.0			pH 6.5		
	d10	d50	d90	d10	d50	d90	d10	d50	d90
CAR	n.m.	n.m.	n.m.	n.m.	n.m.	n.m.	8.99± 0.14	36.75± 0.34	87.98± 0.74
NAP	5.70± 0.28	20.42± 0.79	45.71± 1.07	7.29± 0.75	22.67± 3.36	72.35± 10.48	16.04± 2.91	59.05± 9.84	123.19± 13.85
PIMO	6.99± 0.76	27.76± 4.43	110.00± 11.67	26.60± 3.32	165.76± 17.89	492.60± 27.03	6.74± 0.12	15.70± 0.38	64.86± 16.58

n.m. - not measured

4.2.1.1. Carbamazepine

The solubility of CAR, as a neutral compound, is independent of pH. Furthermore, both ionizable excipients (SLS and SBEβCD) are completely in ionized form across all the tested pH values due to their strongly acidic sulfonic acid groups. Consequently, the experiments were performed only at pH 6.5 [19]. The equilibrium solubility of the molecule was 292.04 ± 4.88 μg/mL, which shows a good correlation with literature data [109,123]. This value was used as a reference for evaluating the impact of the excipients, with statistical significance defined as $p < 0.05$. The equilibrium solubility data with different excipients are shown in Fig. 19.

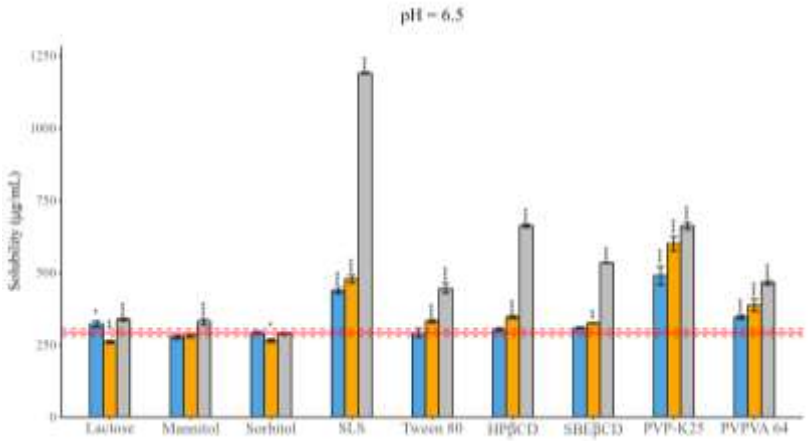

Figure 19. Effect of excipients on the solubility of CAR at three mass ratios in pH 6.5 BRB solution (columns: blue: 1:0.5, orange 1:1, grey 1:3 API: excipient mass ratio; red line: solubility of CAR without excipients; red dashed line: error bars depict 95% confidence intervals for each bar as opposed to sample); p values are the follows *** <0.001, ** 0.01-0.001, * 0.01-0.05

In case of fillers mixed effects were observed, for which concentration dependence was not so obvious. Lactose and mannitol resulted in solubility enchantment, while sorbitol did not have a notable impact or slightly reduced solubility. The solubilizing effect of SLS was more pronounced under all circumstances compared to Tween 80, resulting in a 4-fold increase at 1:3 mass ratio. For CDs, a linear enhancing effect was observed as a function of concentration, although HPβCD complexation at higher concentration was more pronounced (~2-fold) than SBEβCD (~1.5-fold). In the case of polymers PVP-K25 caused a more significant effect than PVPVA 64.

Table 5. represents the results of the Student t-test in the case of the particle size distribution of CAR. The exact values are not shown due to space limitations. In most cases, the excipients cannot inhibit the aggregation of the API in the suspension. The fillers and CDs result in the highest difference, even increasing the particle size 8-fold. Although, in certain cases – especially for surfactants – a decrease can be observed in the particle size.

Table 5. Change in particle size distribution of CAR in the presence of excipients (colours: green: significant increase; red: significant decrease; white: no significant effect on particle size) at pH 6.5. Performed by a student t-test with a 95% significance level.

	SLS			Tween 80			PVP-K25			PVPVA 64			Lactose			Sorbitol			Mannitol			HPβCD			SBEβCD		
	0.5	1	3	0.5	1	3	0.5	1	3	0.5	1	3	0.5	1	3	0.5	1	3	0.5	1	3	0.5	1	3	0.5	1	3
d10	↓	↓	↓	-	-	↓	↓	↑	↑	-	-	-	↑	-	-	↓	↓	-	↓	-	-	-	↓	-	-	↑	↑
d50	↓	↓	↓	↓	↓	↓	↓	↑	↑	-	-	↓	↑	↑	↑	↑	↑	↑	-	↑	↑	↓	↓	↑	↑	↑	↑
d90	-	↓	↓	↓	↓	↓	↓	↑	↑	↑	↑	↓	↑	↑	↑	↓	↑	↑	↑	↑	↑	↑	↑	↑	↑	↑	↑

4.2.1.2. Naproxen

The equilibrium solubility of NAP is pH-dependent, due to its ionizable carboxylic acid group [19]. As a result, at pH 6.5, where nearly 99% of the molecule is in anionic form, the solubility of NAP is ~400-times higher compared to that of its neutral form, which is dominant at pH 3.0. The equilibrium solubility values of NAP were the following: 8.45±0.41 µg/mL (pH 3.0); 171.97±7.48 µg/mL (pH 5.0); 3791.55±63.07 µg/mL (pH 6.5). These values show a good correlation with literature data [19]. The results are illustrated in Fig. 20.

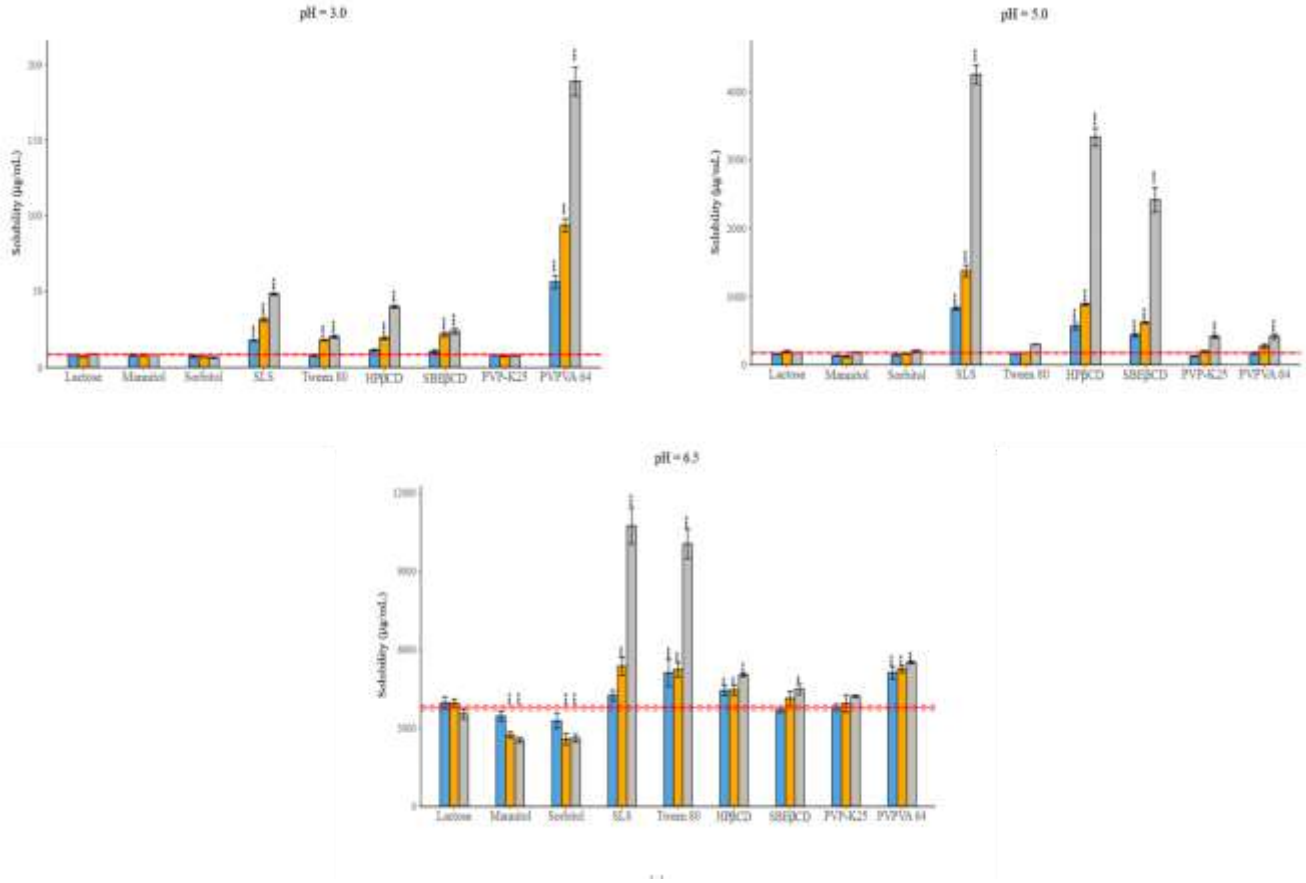

Figure 20. Effect of excipients on the solubility of NAP at three mass ratios in pH 3.0; pH 5.0 and pH 6.5 BRB solution (columns: blue: 1:0.5, orange 1:1, grey 1:3 API: excipient mass ratio; red line: solubility of NAP without excipients; red dashed lines: error bars depict 95% confidence intervals for each bar as opposed to sample); p values are the follows *** <0.001, ** 0.01-0.001, * 0.01-0.05

The impact of different excipients depends on the ionization state of the API. In the case of fillers, lactose did not cause any change in either case. Yet, sugar alcohols cause a decrease in solubility by interacting the ionic form that becomes more prominent with

increasing pH. The solubilizing effect of Tween 80 is lower than SLS under all circumstances. Also, in most cases SLS results in the highest solubility enhancement, except at pH 3.0, where the PVPVA 64 co-polymer reaches a nearly 20-fold increase in solubility compared to the reference. On the other hand, the impact of PVP-K25 is negligible, only causing a significant effect at pH 5.0 at its highest concentration. For CDs, HPβCD showed a more significant effect than SBEβCD, although their effect is more pronounced at higher concentrations.

Table 6. illustrates the results of the statistical analysis of particle size distribution of NAP. At pH 6.5, where the molecule is in anionic form the excipients did not affect or decrease the particle size of the compound. A possible reason can be that the negative charge of the molecule causes a decreased tendency to aggregation. In the presence of the neutral form, the polymers and the Tween 80 can stabilize the molecules in a smaller particle size.

Table 6. Change in particle size distribution of NAP in the presence of excipients (colours: green: significant increase; red: significant decrease; white: no significant effect on particle size). Performed by a student t-test with a 95% significance level.

		SLS			Tween 80			PVPK-25			PVPVA 64			Lactose			Sorbitol			Mannitol			HPβCD			SBEβCD		
		0.5	1	3	0.5	1	3	0.5	1	3	0.5	1	3	0.5	1	3	0.5	1	3	0.5	1	3	0.5	1	3	0.5	1	3
pH3	d10	↑	↑	↑	↓	↓	↓	↓	↓	↓	↓	↓	↓	-	↑	↑	↑	↑	-	↑	-	-	-	-	-	-	-	-
	d50	↑	↑	↑	↓	↓	↓	↓	↓	↓	↓	↓	↓	↑	↑	↑	↑	-	↑	↑	-	-	-	-	↑	↑	↑	↑
	d90	↑	↑	↑	↓	↓	-	↓	↓	↓	↓	↓	↓	↑	↑	↑	↑	↑	-	↑	-	-	-	-	↑	↑	↑	↑
pH5	d10	↑	-	↑	↓	↓	-	-	-	-	-	-	-	-	-	-	-	-	-	-	-	-	-	-	↑	↑	-	-
	d50	↑	↓	↑	↓	↓	↓	↓	-	↑	↓	↓	-	-	-	↓	↓	↑	↑	↓	↓	↓	-	-	↑	↑	↓	-
	d90	↑	↑	↑	↓	↑	↑	↑	↑	↑	↑	↑	↑	-	-	↓	-	-	↓	↓	↓	↓	-	-	-	↑	↓	↑
pH6.5	d10	↓	-	↓	↓	↓	↓	↓	↓	↓	↓	↓	↓	-	-	-	-	-	↓	-	↓	↓	-	-	-	↓	-	↓
	d50	↓	↑	↓	↓	-	↓	↓	↓	↓	↓	↓	↓	-	-	↓	-	-	↓	-	↓	↓	-	-	↑	↓	-	↓
	d90	-	↑	-	↓	-	↓	↓	↓	↓	↓	↑	↓	↑	-	-	-	-	↓	-	-	↓	↑	-	↑	-	↑	↓

4.2.1.3. Pimobendan

Similarly to NAP, the solubility of PIMO also shows pH-dependence [19]. As a weak base (pK_a 4.3), PIMO achieved its highest solubility at pH 3.0, namely 11.46±0.30 µg/mL. As the pH increased, the proportion of the neutral form also increased, leading to a decreased solubility: 0.85±0.04 µg/mL at pH 5.0 and 0.28±0.01 µg/mL at pH 6.5, where the molecule[97]. Fig. 21. illustrates the effect of excipients on thermodynamic solubility.

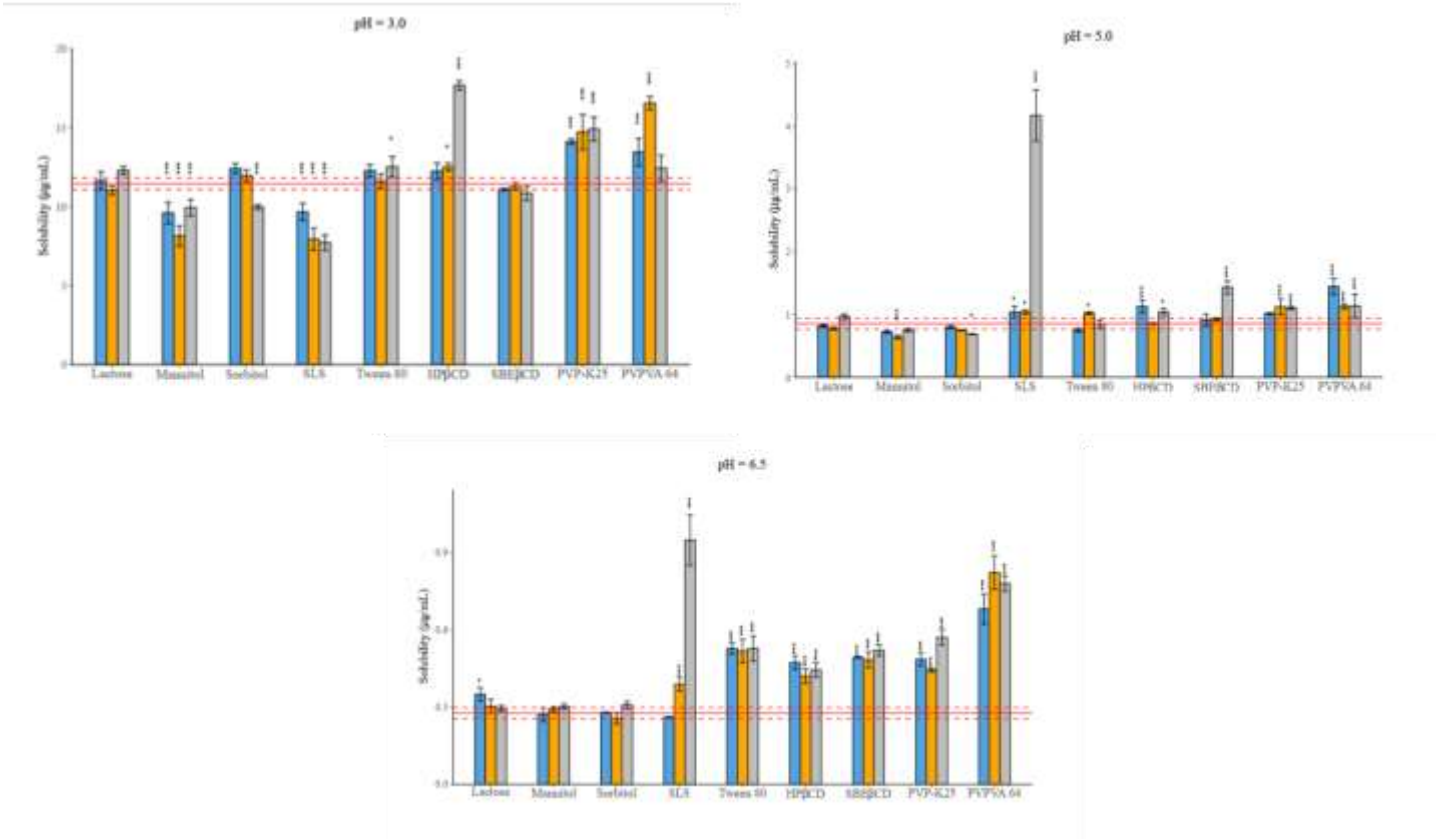

Figure 21. Effect of excipients on the solubility of PIMO at three mass ratios in pH 3.0; pH 5.0 and pH 6.5 BRB solution (columns: blue: 1:0.5, orange 1:1, grey 1:3 API: excipient mass ratio; red line: solubility of PIMO without excipients; red dashed lines: error bars depict 95% confidence intervals for each bar as opposed to sample); p values are the follows *** <0.001, ** 0.01-0.001, * 0.01-0.05

For fillers, lactose did not affect solubility significantly, while mannitol and sorbitol showed a mixed effect, which was more emphasized in the presence of the ionic form. In the case of surfactants, the effect of SLS was more pronounced than that of Tween 80, similarly to NAP. Although at pH 3.0, where the protonated form was dominant, SLS decreased the solubility by nearly 30% at the highest concentration. For CDs, HPβCD affects solubility more than SBEβCD. As with polymers, the effect of PVPVA 64 is more significant than that of PVP-K25, especially in the presence of the neutral form, although the enhancement in solubility is significantly smaller (~ 3-fold) than what is observed with NAP.

Table 7. represents the results of the statistical analysis for the particle size distribution of PIMO. In the presence of ionic form, the dominant change is aggregation, while at pH 5.0, where both the neutral and ionic forms are present, a decrease in particle size is observed in all cases. At pH 6.5 a similar tendency for NAP can be observed, the

polymers and Tween 80 cause a significant decrease in the particle size, while others cause aggregation or did not affect it.

Table 7. Change in particle size distribution of PIMO in the presence of excipients (colours: green: significant increase; red: significant decrease; white: no significant effect on particle size). Performed by a student t-test with a 95% significance level.

		SLS			Tween 80			PVPK-25			PVPVA 64			Lactose			Sorbitol			Mannitol			HPβCD			SBEβCD		
		0.5	1	3	0.5	1	3	0.5	1	3	0.5	1	3	0.5	1	3	0.5	1	3	0.5	1	3	0.5	1	3	0.5	1	3
pH3	d10	↑	↑	-	↑	↑	-	-	-	-	↑	-	↑	↑	-	-	-	-	-	-	-	-	-	-	-	-	-	-
	d50	↑	↑	↑	↑	↑	↑	↑	↑	↑	-	↑	↑	↑	↑	↑	-	-	↑	↓	-	-	-	-	-	↓	↓	↑
	d90	↑	↑	-	↑	↑	↑	↑	↑	-	↑	↑	↑	↑	↑	↑	-	-	-	-	-	↓	-	-	-	↑	-	↑
pH5	d10	↑	-	↓	↓	↓	↓	-	↓	↓	↓	↓	↓	↓	↓	↓	↓	↓	↓	↓	↓	↓	↓	↓	↓	↓	↓	↓
	d50	-	↓	↓	↓	↓	↓	↓	↓	↓	↓	↓	↓	↓	↓	↓	↓	↓	↓	↓	↓	↓	↓	↓	↓	↓	↓	↓
	d90	-	↑	↓	↓	↓	↓	↓	↓	↓	↓	↓	↓	↓	↓	↓	↓	↓	↓	↓	↓	↓	↓	↓	↓	↓	↓	↓	↓
pH6.5	d10	↓	↓	↓	↓	↓	↓	↓	↓	↓	↓	↓	↓	↑	-	-	↑	↑	↑	↑	↑	-	-	-	-	-	↑
	d50	↓	-	↑	↓	↓	↓	↓	↓	↓	↓	↓	↓	↑	-	↑	↑	↑	↑	↑	↑	↑	-	-	↑	-	↑	↑
	d90	-	↑	↑	↑	-	-	-	↑	↓	-	-	-	↑	↓	↑	↑	↑	↑	↑	↑	↑	↑	-	↑	-	↑	↑

4.2.2. Effect of pharmaceutical excipients on GI permeability

The PAMPA method was used to determine P_e, and to study the impact of additives on the permeability of our model compounds under the same conditions as in the case of solubility measurements. According to the pH-partition hypothesis, the transport across the phospholipid bilayer by passive diffusion is favourable for the neutral form of the molecules [19].

4.2.2.1. Carbamazepine

Measured at pH 6.5, the permeability of CAR was found to be 261.38±16.20 10^{-6} cm/s. As demonstrated in Fig. 22. the presence of excipients had a moderate impact on permeability.

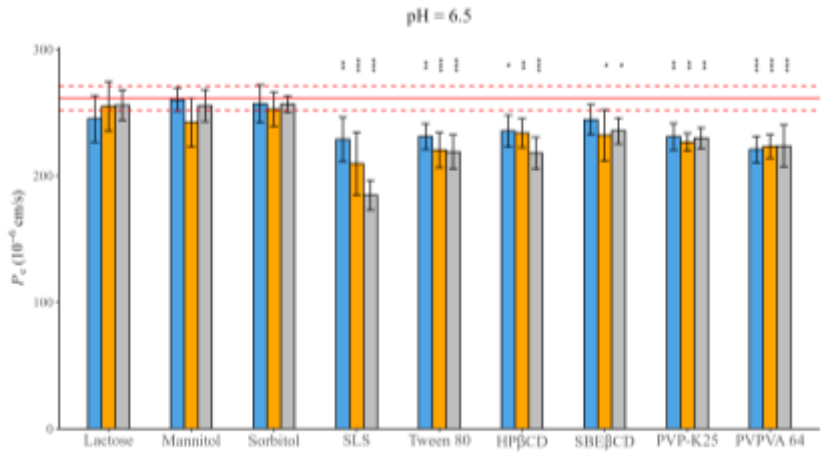

Figure 22. Effect of excipients on the P_e of CAR at three mass ratios in pH 6.5 BRB solution (columns: blue: 1:0.5, orange 1:1, grey 1:3 API: excipient mass ratio; red line P_e of CAR without excipients; red dashed lines: error bars depict 95% confidence intervals for each bar as opposed to sample); p values are the follows *** <0.001, ** 0.01-0.001, * 0.01-0.05

No significant change was observed in the presence of fillers, whereas a decrease in permeability occurred with other excipients. The most significant reduction was induced by SLS, where the concentration dependence on the extent of decrease was pronounced. In contrast, for other additives, no proportional relationship was observed between concentration and the extent of permeability reduction.

4.2.2.2. Naproxen

The permeability of NAP, similarly to its solubility, shows pH-dependence. The highest permeability was observed at pH 3.0, namely 997.62±46.95 10^{-6} cm/s, where nearly 99% of the molecule is in neutral form. With increased ionized fraction at higher pH, permeability decreased to 496.82±32.41 10^{-6} cm/s at pH 5.0 and 28.92±1.61 10^{-6} cm/s at pH 6.5. Fig. 23. demonstrates the effect of excipients on the permeability of NAP.

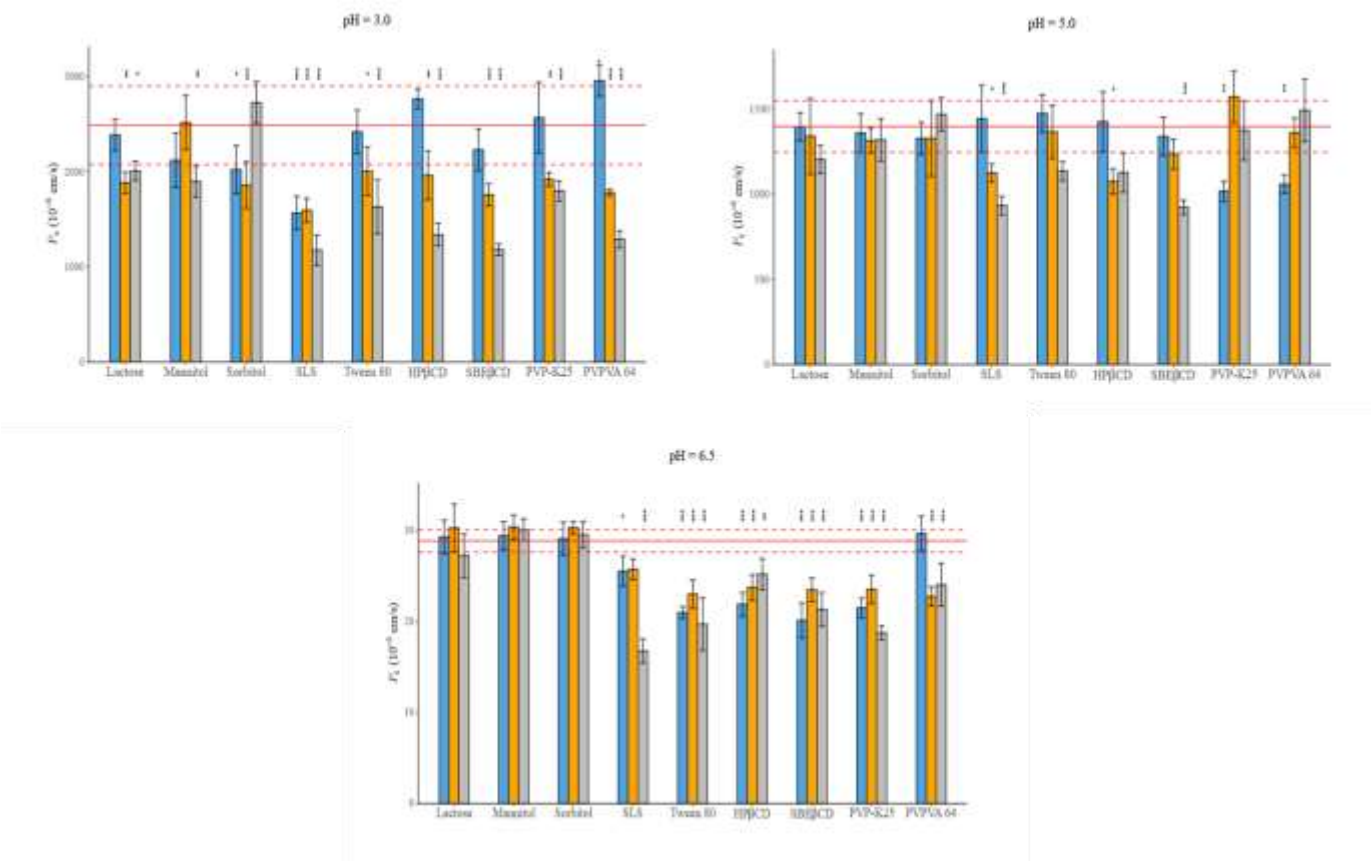

Figure 23. Effect of excipients on the P_e of NAP at three mass ratios in pH 3.0; 5.0 and 6.5 BRB solution (columns: blue: 1:0.5, orange 1:1, grey 1:3 API: excipient mass ratio; red line P_e of NAP without excipients; red dashed lines: error bars depict 95% confidence intervals for each bar as opposed to sample); p values are the follows *** <0.001, ** 0.01-0.001, * 0.01-0.05

The fillers caused a mixed effect, as well as the polymers. In most cases, the effect of lactose is negligible, while for sugar alcohols a decrease in permeability can be detected, especially in the presence of the neutral form. A similar trend can be observed in the case of polymers, where PVP-K25 caused a nearly 30% and PVPVA 64 a nearly 50% decrease in permeability at pH 3.0 at their highest concentration. While in the case of PVP-K25, this trend is similar at pH 6.5, where the molecule is fully ionized, the permeability-reducing effect of PVPVA 64 is moderate, only ~20% under the same circumstances. For CDs, the impact of SBEβCD is more pronounced, reducing permeability by 10-15% more than HPβCD. As with solubility, the effect of SLS on permeability was the most pronounced, resulting in a nearly 50% decrease in permeability at its highest concentration at all pH values.

4.2.2.3. Pimobendan

PIMO, as a basic compound, achieved its maximum permeability at pH 6.5, namely 339.67±20.26 10^{-6} cm/s, followed by 274.82±16.13 10^{-6} cm/s at pH 5.0 and the lowest at pH 3.0, only 12.00±1.42 10^{-6} cm/s. Fig. 24. represents the effect of excipients on the permeability of PIMO.

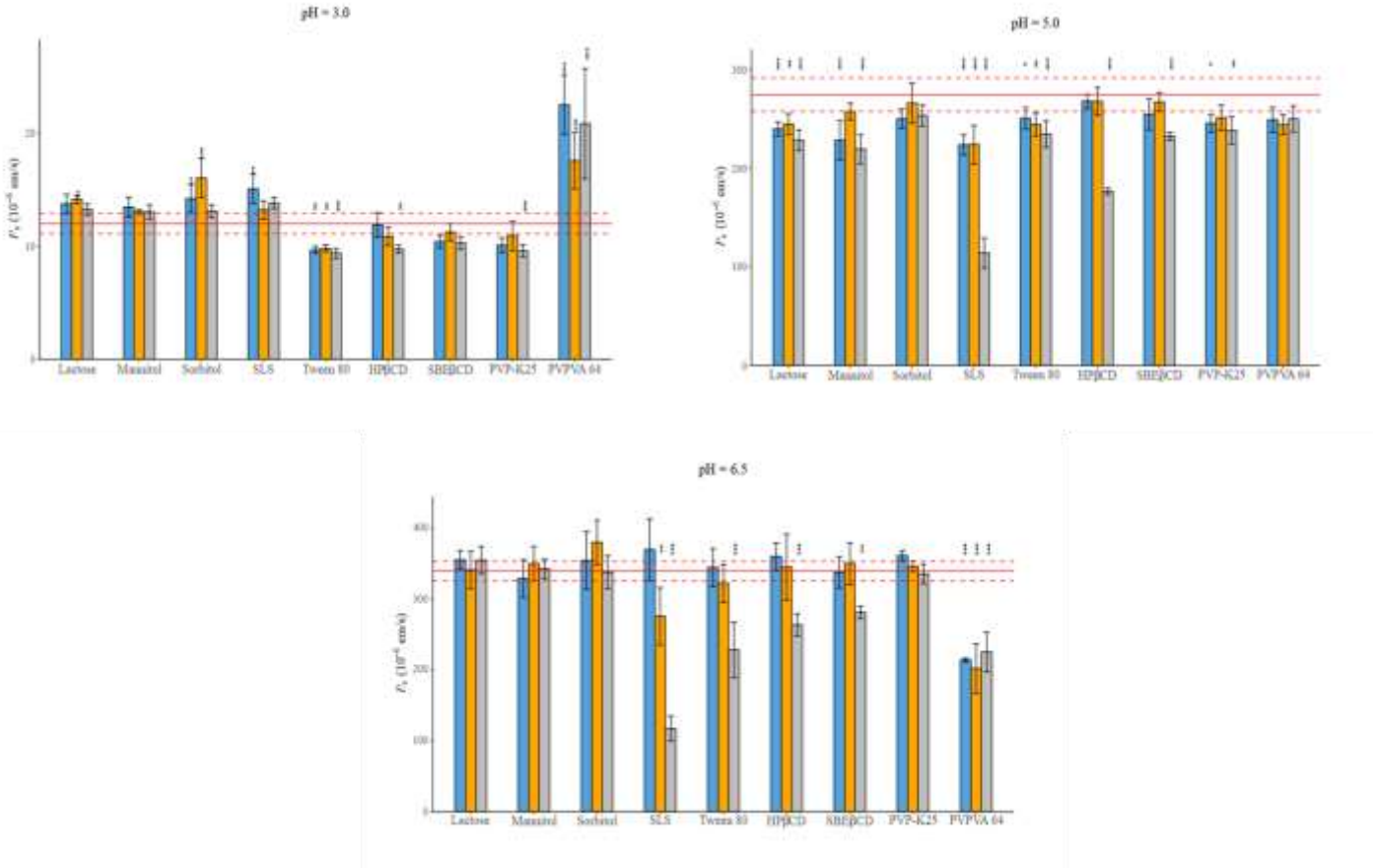

Figure 24. Effect of excipients on the P_e of PIMO at three mass ratios in pH 3.0; 5.0 and 6.5 BRB solution (columns: blue: 1:0.5, orange 1:1, grey 1:3 API: excipient mass ratio; red line P_e of PIMO without excipients; red dashed lines: error bars depict 95% confidence intervals for each bar as opposed to sample) p values are the follows *** <0.001, ** 0.01-0.001, * 0.01-0.05

For fillers, lactose did not significantly affect the P_e of the molecule, the sugar alcohols cause a mixed effect, like in the case of NAP. This trend is also observed with polymers; however, PVP-K25 displays a limited effect that becomes significant only at its highest concentration. Meanwhile, for PVPVA 64 an interesting effect can be noticed. At pH 3.0, where the molecule exists in its ionized form, a nearly 1.5-fold increase in permeability can be detected, while at pH 6.5, where the compound is fully unionized, a similar decrease is observed. In the case of PIMO, in contrast to NAP, the permeability-

reducing effect of HPβCD is more pronounced than that of SBEβCD. Tween 80 causes a moderate decrease in permeability compared to SLS, which achieves ~60-70% reduction in permeability at higher pH values. Yet, at pH 3.0 an exception can be observed, because SLS did not significantly affect permeability, while Tween 80 results in a nearly 20% decrease in P_e.

5. Discussion

5.1. Impact of different solvents on transdermal permeability

5.1.1. Effect of solvents on PAMPA membrane integrity

The developed simple method was suitable for testing the integrity of the artificial membrane. No solvent effect was detected on visual observation of the plate wells. Results of the standard permeability test on pre-treated plates with a reference compound, piroxicam, fitted well with previously reported data. Naturally, the P_e value of piroxicam was slightly increased on the pre-treated membranes, potentially due to piroxicam (log*P* 1.71) partitioning into the remaining solvent film on the membrane, thereby increasing the surface concentration. However, the variability in permeability was low, supporting the fact that the membrane remained structurally intact.

5.1.2. Effect of solvents on Skin-PAMPA permeability of PER

The study was focused on the behaviour of the Skin-PAMPA membrane when an apolar compound was dissolved in various solvents widely used in cosmetics. PER served as a good model compound, being UV active for direct plate reader detection and reasonably soluble in the studied 13 solvents (9 pure and 4 mixtures). The selected 6 h incubation time in each case allowed the HT evaluation. The permeability of PER was significantly affected by the solvent in which it was dissolved, with a change of about 1.5 orders of magnitude. The method effectively differentiated the permeability values, enabling categorization into high, medium, and low classes.

During the measurements, some limitations of this method have been established. Applying viscous solvents can be challenging because the application of solvents to the PAMPA plate is a time-consuming process, so correction for the time factor needs to be implemented during the evaluation of the results. The tension of the solvents can also be a limiting factor, since the concentration of high-tension solutions can change during the experiment, leading to invalid permeability results. Finally, permeation values of the investigated compound cannot be too high or too low, because in these cases the method is not suitable for the measurement.

5.1.3. Permeation kinetics of PER across pig ear skin

The Skin-PAMPA model was compared with permeation measurements performed on pig skin to investigate its applicability as a screening tool for modelling transdermal permeation. Permeation potential can be described in multiple ways: the permeated amount in a finite time (Qt), the flux (J), which denotes the average rate of mass transfer across the membrane, and the permeability coefficient (P_m or K_p), which characterizes the penetration rate through the membrane. Consequently, permeability data from Skin-PAMPA and the pig skin model were compared to identify the most suitable parameter for differentiating solvent-dependent permeability.

In the case of flux, poor correlation can be observed. A better correlation can be detected between the permeated amounts (AUC_{PAMPA} vs. $Qt_{pig\ skin}$), because they are normalized to the donor concentration, yet there were two outliers. The best correlation was achieved when the logarithm of permeability coefficients was compared, because these values are independent of the donor concentration. The most significant differences were observed in the case of ethanol (S2) and dimethyl isosorbide (S4). A possible reason is that the API and the solvent together disrupted the PAMPA membrane, which resulted in a higher permeability. This effect was less emphasized when these solvents were in a low ratio in a water-containing mixture (e.g. S6 and S5). Although, a comprehensive understanding still necessitates additional investigations.

Skin-PAMPA consists of a single membrane, while the native pig skin is a complex, multiple layered, 700-1200 μm thick membrane. Due to this, the flux and the permeability values were higher in the case of Skin-PAMPA, than pig skin. This can also explain the lower relative standard deviation of PAMPA results compared to pig skin [124].

5.2. Effects of pharmaceutical excipients on solubility, GI permeability and their relationship

The influencing effect of different excipients on ionizable APIs depends on the ionization state of the latter. In general, the most significant changes in the measured parameters were observed in the presence of the neutral form of the APIs, except for sugar alcohols.

Fig. 25. illustrates the effects of excipients as percentage differences compared to the reference for both parameters (the effect of lactose was negligible, so it is not shown).

The modification of the solubility of the molecules influences their permeability. In the following discussion, we evaluate four different groups of excipients - namely fillers, cyclodextrins, surfactants and polymers - and their effect on both parameters.

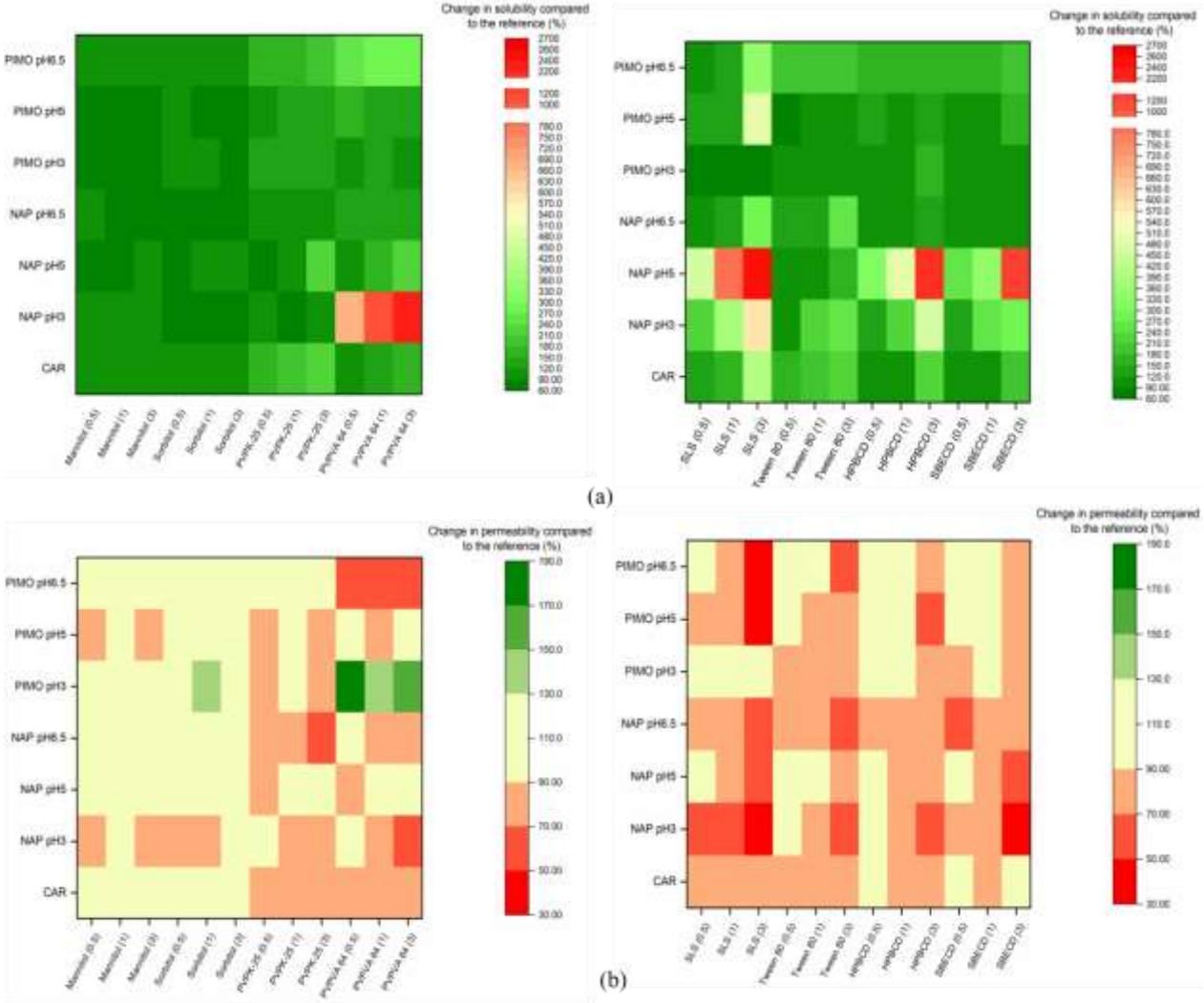

Figure 25. (a) Change in solubility compared to the reference, expressed as a percentage (b) Change in permeability compared to the reference, expressed as a percentage

5.2.1. Fillers

Lactose did not or only slightly affects the investigated parameters. However, sugar alcohols resulted in a mixed effect, which is more pronounced in the presence of the ionic form of the API. It may be attributed to their hydrotropic properties. Hydrotropic agents can influence solubility via various mechanisms, such as self-aggregation or the depression of water activity [104,125]. For sugar alcohols, the latter seems probable [126]. However, to achieve a solubilizing effect, the hydrotropic agents need to be applied in high concentrations due to their higher hydrophilic/lipophilic balance [126]. In our

study, the highest tested concentration did not reach 10 w/v%, which may explain why the solubility of the neutral form did not show significant improvement, whereas a reduction of solubility was observed in the presence of the ionic form. A possible reason is that mannitol and sorbitol increase the strength of hydrogen bonds among water molecules, making the solvent less polar [125,126]. This leads to a reduced solubility in the case of the hydrophilic ionic form. In contrast, in the case of permeability, their impact is more pronounced in the presence of the neutral form. These findings show a good correlation with literature data [127,128].

5.2.2. Cyclodextrins

Based on the solubility results, the solubilizing effect of HPβCD was more significant compared to SBEβCD. A significant enhancement in solubility – about 20-fold – was observed with NAP, whereas the other two APIs demonstrated only a 2- to 3-fold enhancement. For CAR, these findings show a good correlation with literature data, as reported by *Volkova et al.*, where CDs were also applied in low concentrations [129,130]. For NAP, due to its smaller molecular size a better complexation can be achieved. Furthermore, it is negatively charged at higher pH values, which can lead to electrostatic repulsion, reducing the stability of its complex with SBEβCD [131]. The importance of molecular size is also supported by the fact that although PIMO can be positively charged, SBEβCD did not cause a more significant solubility improvement than HPβCD.

In the case of permeability measurements, a mixed effect of these excipients can be observed. Generally, the permeability-reducing effect is more pronounced at higher concentrations due to the ability of CDs to form inclusion complexes and through this mechanism decrease the free fraction of the APIs [104,105]. In lower concentrations, CDs did not affect permeability. Based on the literature, in certain cases CDs can cause a permeability enhancement. One potential mechanism is the faster transport through the UWL via the inclusion complex or possibly the complex formation with membrane cholesterol [106,107].

5.2.3. Surfactants

Surfactants are commonly used solubilizing excipients, which enhance solubility via micelle formation with various CMC values. The non-ionic Tween 80 has a lower CMC (0.012-1.05 mM), than the anionic SLS (8.06-8.57 mM). However, above the CMC the solubilizing effect of SLS is more significant than that of Tween 80. The lower solubilizing capacity of Tween 80 can be attributed to its larger molecular size and its ability of self-aggregation [132,133]. These aggregates can limit the micelle formation with the APIs. For instance, in the presence of SLS, CAR and PIMO reach a 4-fold, while NAP can achieve a 20-fold (at pH 5.0) solubility enhancement at a 1:3 mass ratio. Tween 80 provides an approximately 1.5–2-fold increase under the same conditions. Due to it, the permeability-reducing effect of Tween 80 is less emphasized than that of SLS. While Tween 80 can cause a 20-35% reduction in permeability, it is more pronounced in the presence of the neutral form in the case of ionizable molecules. Under the same conditions, SLS can achieve even a 60% decrease in permeability. The reason for the decrease in permeability is the reduction of the concentration of free fraction, which is capable of penetrating the membranes, through micelle formation [104]. These findings show a good correlation with the study of *Li et al.* [132], who investigated the effect of these two surfactants on carbamazepine-nicotinamide co-crystals, and *Tőzsér et al.* [97], who identified similar tendency in the case of PIMO and SLS. An interesting exception can be observed with SLS in the case of PIMO at pH 3.0, where a significant solubility-reducing effect – nearly 33% – was detected. A possible reason may be the formation of poorly soluble lauryl sulfate salts. A similar finding was reported by *Bhattachar et al.* [134]. Due to this a 10% improvement on permeability can be observed.

5.2.4. Polymers

Polymers can perform several functions in drug formulations, such as emulsifying agent, coating agent, binder, etc [135]. Furthermore, polymers in certain cases can improve the equilibrium solubility by stabilizing the solute API molecules at a higher concentration.

The impact of PVPVA 64 was, in almost all cases, more pronounced than PVP-K25. CAR made an exception, because PVP-K25 shows a higher solubilizing effect in this case, yet during the permeability measurements, the two polymers caused a similar

decrease of permeability. In the case of NAP and PVP-K25 our findings show a good correlation with the results of *Bolten et al.* [136], indicating that PVP polymers do not influence the solubility of NAP. The better effect of PVPVA 64 may be attributed to its copolymer structure, where the hydrophobic vinyl acetate units decrease its overall hydrophilicity compared to PVP-K25, giving PVPVA 64 a slightly amphiphilic character. Consequently, PVPVA 64 was observed to be suitable for micelle formation. This may also be one of the reasons for its better solubilizing effect [137,138]. In the case of NAP, PVPVA 64 reached an extremely high value, where the solubility enhancement was nearly 22-fold in the presence of the neutral form [139]. For PIMO, the solubilizing effect was also better in the case of the non-ionized form, although it achieves only a 4-fold increase in solubility. This supports the fact that the acid-base character of the APIs is particularly important in the solubility-improving effect of polymers, as emphasized by *Fornells et al.* [140].

The impact of polymers on permeability, just as on solubility, is highly dependent on the ionization state of the APIs. In the case of PIMO at pH 3.0, where the ionic form of the molecule is dominant, PVP-K25 resulted in around a 15% decrease in permeability, while PVPVA 64 reached a nearly 1.5-fold increase. Whereas, in the presence of the neutral form, a reversed effect can be observed: PVP-K25 did not significantly affect the permeability, while PVPVA 64 resulted in a decrease of about 35%. However, the concentration dependence of the impact is not so obvious. For NAP a significant decrease, around 50% can be observed at a pH where the neutral form dominates. This shows a good correlation with the solubility-enhancing effect. In the presence of the anionic form, the effect of PVP-K25 is more pronounced. This is probably due to the various interactions between the polymers and the model compounds, which include both polar and hydrophobic ones [140,141].

6. Conclusions

The investigation of the applicability and limitations of HTS techniques is essential for supporting drug development. Also, studying the correlation between permeability and solubility, two critical parameters of absorption, in the presence of different excipients, is important during formulation optimization.

My primary objective was to investigate the applicability of the Skin-PAMPA technique as a screening tool for non-polar compounds dissolved in various solvents. PER was selected as a model compound, and 13 solvents with varying polarities, along with solvents mixtures, mostly used in the cosmetic sector, were tested.

Initially, a membrane integrity test was developed to examine the direct impact of the solvents on the membrane. Since no membrane damage was observed, the measurements were performed in infinite dose of the API.

The results indicate that Skin-PAMPA is a reliable method for HT measurement of permeability of APIs dissolved in a diverse range of solvent types, from extremely polar to highly non-polar, including their mixtures. The results enable the classification of PER permeability into 3 categories: high, medium, and low.

Ex vivo Franz-cell measurements were also carried out on porcine ear skin for nine solvents to compare with PAMPA permeability. The aim was to identify the optimal parameter for correlating *in vitro* and *ex vivo* data. The permeability coefficient ($\log P_m$ or $\log K_p$) was determined in this analysis to be the most suitable parameter (with a correlation coefficient R^2=0.844), as it is independent of the donor concentration. This is particularly crucial for comparing the permeability of compounds with significant differences in solubility.

Our findings support the utilization of Skin-PAMPA as a screening tool to predict transdermal permeability from various solvents in the early stage of drug development.

The second part of my study focused on the effect of nine pharmaceutical excipients (fillers, CDs, surfactants, and polymers) on equilibrium solubility and intestinal permeability, as the two key factors of drug absorption, in the case of three BCS II model compounds (CAR, NAP, PIMO) at three different mass ratios.

Initially, we established a complete, experimentally measured database for these two parameters, comprising 196 equilibrium solubility values derived from 474 measurements performed by a validated SSF method and 196 permeability values

obtained from the PAMPA method, encompassing 1141 experimental points. These pieces of data enable us the elucidation of the impact of excipients on solubility and permeability of the three studied drugs. Moreover, we demonstrated that the solubility-permeability interplay is a critical factor to be considered in the formulation design. Furthermore, our investigation enabled the evaluation of multiple influencing factors.

Firstly, the structure of the APIs, such as NAP, which facilitates many molecular interactions, can attain a solubility enhancement of up to 20-fold, but the absorption characteristics of CAR, owing to its rigid ring system, can be altered only in a rather modest degree. However, flexible structural elements may restrict the interactions between the API and the excipients, likely accounting for PIMO's attainment of just a 3.5 to 4-fold improvement in solubility.

Secondly, we may analyse the influence of the ionization state of APIs on the effect of excipients. The effect of excipients on NAP and PIMO was significantly more pronounced in the neutral form compared to the ionized form, particularly in the presence of polymers.

Finally, we can conclude that the optimal excipient selection enhances solubility while minimalizing any adverse effects on permeability. Our research supports optimal selection in the early stages of drug development by providing a comprehensive understanding of the effects of additives.

7. Summary

The first part of this work investigates the applicability of the Skin-PAMPA method in the case of non-polar APIs, using PER as a model compound, dissolved in 13 solvents and solvent mixtures of different polarity. At first, an easily conducted membrane integrity test has been developed to check the effect of the solvents on the membrane without the API. The membrane was pre-treated with the solvents for 7 hours, then the solvents were removed, and a standard measurement was performed with a reference compound. There was no significant difference compared to the literature data, and the low standard deviations show the reliability of the method. As comparison, *ex vivo* pig ear skin measurements were conducted to find the best parameter to correlate the two models. This parameter was the permeation coefficient, due to its independence of the donor concentration. Our results supported the use of Skin-PAMPA as a screening tool. However, during the measurements, some limitations have been observed, such as the viscosity or the tension of the solvents, which need to be considered when designing the measurement.

The second part of this work was studying the effect of nine pharmaceutical excipients (fillers, CDs, surfactants, and polymers), commonly used in oral formulations, on the equilibrium solubility and intestinal permeability of three APIs (CAR, NAP, PIMO) with different acid-base properties. The impact of pH and the additive concentration on the interactions between the APIs and excipients was also investigated. For the ionizable compounds it can be stated that the impact of additives is more pronounced in the presence of the neutral form, especially in the case of polymers. During our work, it was possible to examine the solubility-permeability interplay in detail. Among fillers, lactose is the most inert one. CDs can improve solubility, while permeability is not always affected. Also, HPβCD is a better option over SBEβCD in most cases. The solubility-enhancing effect of surfactants is more pronounced, they also decrease permeability to a higher degree. However, Tween 80 can be a more suitable alternative to SLS at higher concentrations because its impact on reducing permeability is comparatively lower. The effect of PVPVA 64 on both parameters is more favourable than PVPK-25. Our work provides a comprehensive overview of the impact of excipients on solubility-permeability interplay and emphasizes the importance of optimal excipient selection in the early stages of drug development.

8. References

1. Hugo Kubinyi *(Editor)* 3D QSAR in Drug Design. *Springer Dordrecht* **1998**; ISBN: 9780792347903
2. Chandershekar, A; Bhaskar, A; Mekkanti ManasaRekha; Rinku Mathappan. A Review on Computer Aided Drug Design (CAAD) and It's Implications in Drug Discovery and Development Process. *IJHCBS* **2020**, *1*, 27-33.
3. Zoran Mandić Physico-Chemical Methods in Drug Discovery and Development. *IAPC* **2014**, ISBN: 9789535694212.
4. Liu, R.; Li, X.; Lam, K.S. Combinatorial Chemistry in Drug Discovery. *Curr Opin Chem Biol* **2017**, *38*, 117–126.
5. Mak, K.K.; Pichika, M.R. Artificial Intelligence in Drug Development: Present Status and Future Prospects. *Drug Discov Today* **2019**, *24*, 773–780.
6. Kawabata, Y.; Wada, K.; Nakatani, M.; Yamada, S.; Onoue, S. Formulation Design for Poorly Water-Soluble Drugs Based on Biopharmaceutics Classification System: Basic Approaches and Practical Applications. *Int J Pharm* **2011**, *420*, 1–10.
7. Lennernäs, H.; Aarons, L.; Augustijns, P.; Beato, S.; Bolger, M.; Box, K.; Brewster, M.; Butler, J.; Dressman, J.; Holm, R.; Julia Frank, K.; Kendall, R.; Langguth, P.; Sydor, J.; Lindahl, A.; McAllister, M.; Muenster, U.; Müllertz, A.; Ojala, K.; Pepin, X.; Reppas, C.; Rostami-Hodjegan, A.; Verwei, M.; Weitschies, W.; Wilson, C.; Karlsson, C.; Abrahamsson, B. Oral Biopharmaceutics Tools - Time for a New Initiative - An Introduction to the IMI Project OrBiTo. *Eur J Pharm Sci* **2014**, *57*, 292–299.
8. Wilson, C.G.; Aarons, L.; Augustijns, P.; Brouwers, J.; Darwich, A.S.; De Waal, T.; Garbacz, G.; Hansmann, S.; Hoc, D.; Ivanova, A.; Koziolek, M.; Reppas, C.; Shick, P.; Vertzoni, M.; Arturo García-Horsman, J. Integration of Advanced Methods and Models to Study Drug Absorption and Related Processes: An UNGAP Perspective. *Eur J Pharm Sci* **2022**, *172,* 106100.
9. Jain, K.K. An Overview of Drug Delivery Systems. *Methods Mol Biol* **2020**, *2059*, 1–54.
10. Alqahtani, M.S.; Kazi, M.; Alsenaidy, M.A.; Ahmad, M.Z. Advances in Oral Drug Delivery. *Front Pharmacol* **2021**, *12*, 618411.

11. Homayun, B.; Lin, X.; Choi, H.J. Challenges and Recent Progress in Oral Drug Delivery Systems for Biopharmaceuticals. *Pharmaceutics* **2019**, *11*, 129.
12. Ruiz-Garcia, A.; Bermejo, M.; Moss, A.; Casabo, V.G. Pharmacokinetics in Drug Discovery. *J Pharm Sci* **2008**, *97*, 654–690.
13. Piper M. Treuting Comparative Anatomy and Histology, S.M.D.K.S.M., Edition; Second.; Academic Press: London, **2017**.
14. Liedlgruber, M.; Uhl, A.; Liedlgruber Uhl, M.A.; Uhl, A. A Summary of Research Targeted at Computer-Aided Decision Support *in Endoscopy of the Gastrointestinal Tract Technical Report Series*; **2011**.
15. Scratcherd, T.; Grundy, D. The physiology of intestinal motility and secretion. *Br J Anaesth*. **1984,** *56*, 3-18.
16. Locatelli, I.; Nagelj Kovai, N.; Mrhar, A.; Bogataj, M. Gastric Emptying of Non-Disintegrating Solid Drug Delivery Systems in Fasted State: Relevance to Drug Dissolution. *Expert Opin Drug Deliv* **2010**, *7*, 967–976.
17. Lipinski, C.A.; Dominy, B.W.; Feeney, P.J. Experimental and Computational Approaches to Estimate Solubility and Permeability in Drug Discovery and Development Settings. *Adv Drug Deliv Rev* **2001**, *46*, 3-26..
18. Amidon, G.L., L.H., S.V.P., C.J.R. A Theoretical Basis for a Biopharmaceutic Drug Classification: The Correlation of in Vitro Drug Product Dissolution and in Vivo Bioavailability. *Pharm Res* **1995**, *46*, 413–420.
19. Avdeef, A. Absorption and Drug Development: Solubility, Permeability and Charge State; Second.; John Wiley & Sons, Inc., **2012.**
20. Sabbagh, F.; Kim, B.S. Recent Advances in Polymeric Transdermal Drug Delivery Systems. *J Control Release* **2022**, *341*, 132–146.
21. Phatale, V.; Vaiphei, K.K.; Jha, S.; Patil, D.; Agrawal, M.; Alexander, A. Overcoming Skin Barriers through Advanced Transdermal Drug Delivery Approaches. *J Control Release* **2022**, *351*, 361–380.
22. Kushwaha, R.; Palei, N.N. Transdermal Drug Delivery Systems: Different Generations and Dermatokinetic Assessment of Drug Concentration in Skin. *Pharmaceut Med* **2024,** *38*, 407-427.
23. Proksch, E. PH in Nature, Humans and Skin. *J Dermatol* **2018**, *45*, 1044–1052.

24. Jeong, W.Y.; Kwon, M.; Choi, H.E.; Kim, K.S. Recent Advances in Transdermal Drug Delivery Systems: A Review. *Biomater Res* 2021, *25*.
25. Honari, G.; Maibach, H. Skin Structure and Function. In book: *Applied Dermatotoxicology: Clinical Aspects*; Elsevier, **2014**; pp. 1–10 ISBN 9780124201309.
26. Prausnitz, M.R.; Langer, R. Transdermal Drug Delivery. *Nat Biotechnol* **2008**, *26*, 1261–1268.
27. Edward H.Kerns; Li Di *Drug-like Properties: Concepts, Structure Design and Methods: From ADME to Toxicity Optimization*; Elsevier: San Diego, **2008**.
28. Berben, P.; Bauer-Brandl, A.; Brandl, M.; Faller, B.; Flaten, G.E.; Jacobsen, A.C.; Brouwers, J.; Augustijns, P. Drug Permeability Profiling Using Cell-Free Permeation Tools: Overview and Applications. *Eur J Pharm Sci* **2018**, *119*, 219–233.
29. Bareford, L.M.; Swaan, P.W. Endocytic Mechanisms for Targeted Drug Delivery. *Adv Drug Deliv Rev* **2007**, *59*, 748–758.
30. Arnott, J.A.; Planey, S.L. The Influence of Lipophilicity in Drug Discovery and Design. *Expert Opin Drug Discov* **2012**, *7*, 863–875.
31. Knights, K.M.; Stresser, D.M.; Miners, J.O.; Crespi, C.L. In Vitro Drug Metabolism Using Liver Microsomes. *Curr Protoc Pharmacol* **2016**, *74*, 7.8.1-7.8.24.
32. Riley, R.J.; Grime, K. Metabolic Screening in Vitro: Metabolic Stability, CYP Inhibition and Induction. *Drug Discov Today Technol* **2004**, *1*, 365–372.
33. Bhattachar, S.N.; Deschenes, L.A.; Wesley, J.A. Solubility: It's Not Just for Physical Chemists. *Drug Discov Today* **2006**, *11*, 1012–1018.
34. Baka, E.; Comer, J.E.A.; Takács-Novák, K. Study of Equilibrium Solubility Measurement by Saturation Shake-Flask Method Using Hydrochlorothiazide as Model Compound. *J Pharm Biomed Anal* **2008**, *46*, 335–341.
35. Avdeef, A.; Fuguet, E.; Llinàs, A.; Ràfols, C.; Bosch, E.; Völgyi, G.; Verbic, T.; Boldyreva, E.; Takács-Novák, K. Equilibrium Solubility Measurement of Ionizable Drugs - Consensus Recommendations for Improving Data Quality. *ADMET DMPK* **2016**, *4*, 117–178.

36. Lakshmi Narasimham Y S; Vasant D Barhate Kinetic and Intrinsic Solubility Determination of Some B-Blockers and Antidiabetics by Potentiometry. *J Pharm Res* **2011**, *4*, 532536.

37. Box K., Völgyi G., Baka E., Stuart M., Takács-Novák K., Comer J.: Equilibrium vs kinetic measurements of aqueous solubility, and the ability of compounds to supersaturate in solution – a validation study. *J Pharm Sci* **2006**, *95*, 1298–1307.

38. Avdeef, A. Physicochemical Profiling (Solubility, Permeability and Charge State). *Curr Top Med Chem* **2001**, *1*, 277-351.

39. Völgyi, G.; Baka, E.; Box, K.J.; Comer, J.E.A.; Takács-Novák, K. Study of PH-Dependent Solubility of Organic Bases. Revisit of Henderson-Hasselbalch Relationship. *Anal Chim Acta* **2010**, *673*, 40–46.

40. Bergström, C.A.S.; Avdeef, A. Perspectives in Solubility Measurement and Interpretation. *ADMET DMPK* **2019**, *7*, 88–105.

41. Hansen, N.T.; Kouskoumvekaki, I.; Jørgensen, F.S.; Brunak, S.; Jónsdóttir, S.Ó. Prediction of PH-Dependent Aqueous Solubility of Druglike Molecules. *J Chem Inf Model* **2006**, *46*, 2601–2609.

42. E. Galia; E. Nicolaides; D. Hörter; R. Löbenberg; C. Reppas; J. B. Dressman Evaluation of Various Dissolution Media for Predicting in Vivo Performance of Class I and II Drugs. *Pharm Res* **1998**, *15*, 698–705.

43. Jennifer B. Dressman; Gordon L. Amidon; Christos Reppas; Vinod P. Shah Dissolution Testing as a Prognostic Tool for Oral Drug Absorption: Immediate Release Dosage Forms. *Pharm Res* **1998**, *15*, 11.

44. Levis, K.A.; Lane, M.E.; Corrigan, O.I. Effect of Buffer Media Composition on the Solubility and Effective Permeability Coefficient of Ibuprofen. *Int J Pharm* **2003**, *253*, 49–59.

45. Kleberg, K.; Jacobsen, J.; Müllertz, A. Characterising the Behaviour of Poorly Water Soluble Drugs in the Intestine: Application of Biorelevant Media for Solubility, Dissolution and Transport Studies. *J Pharm Pharmacol* **2010**, *62*, 1656–1668.

46. Jantratid, E.; Janssen, N.; Reppas, C.; Dressman, J.B. Dissolution Media Simulating Conditions in the Proximal Human Gastrointestinal Tract: An Update. *Pharm Res* **2008**, *25*, 1663–1676.

47. Takács-Novák, K.; Szoke, V.; Völgyi, G.; Horváth, P.; Ambrus, R.; Szabó-Révész, P. Biorelevant Solubility of Poorly Soluble Drugs: Rivaroxaban, Furosemide, Papaverine and Niflumic Acid. *J Pharm Biomed Anal* **2013**, *83*, 279–285.
48. Makowski, M.; Bogunia, M. Influence of Ionic Strength on Hydrophobic Interactions in Water: Dependence on Solute Size and Shape. *J Phys Chem B* **2020**, *124*, 10326–10336.
49. Serajuddin, A.T.M. Salt Formation to Improve Drug Solubility. *Adv Drug Deliv Rev* **2007**, *59*, 603–616.
50. Carvajal, M.T.; Yalkowsky, S. Effect of pH and Ionic Strength on the Solubility of Quinoline: Back-to-Basics. *AAPS Pharm Sci Tech* **2019**, *20*, 124.
51. Sandri, G.; Bonferoni, M.C.; Ferrari, F.; Rossi, S.; Caramella, C.M. The Role of Particle Size in Drug Release and Absorption. In book: Particulate Products **2014**; pp. 323–341.
52. Letellier, P.; Mayaffre, A.; Turmine, M. Solubility of Nanoparticles: Nonextensive Thermodynamics Approach. *J Phys Condens Matter* **2007**, *19*, 436229.
53. Chawla, G.; Bansal, A.K. A Comparative Assessment of Solubility Advantage from Glassy and Crystalline Forms of a Water-Insoluble Drug. *Eur J Pharm Sci* **2007**, *32*, 45–57.
54. Murdande, S.B.; Pikal, M.J.; Shanker, R.M.; Bogner, R.H. Aqueous Solubility of Crystalline and Amorphous Drugs: Challenges in Measurement. *Pharm Dev Technol* **2011**, *16*, 187–200.
55. Gurunath, S.; Pradeep Kumar, S.; Basavaraj, N.K.; Patil, P.A. Amorphous Solid Dispersion Method for Improving Oral Bioavailability of Poorly Water-Soluble Drugs. *J Pharm Res* **2013**, *6*, 476–480.
56. Szabó Kálmán *Fizikai Kémia*; Semmelweis Egyetem Gyógyszertudományi Kar: Budapest, **1995.**
57. Jagtap, S.; Magdum, C.; Jadge, D.; Jagtap, R. Solubility Enhancement Technique: A Review. *JPSR*, **2018**, *10*, 2205-2211.
58. Nyamba, I.; Sombié, C.B.; Yabré, M.; Zimé-Diawara, H.; Yaméogo, J.; Ouédraogo, S.; Lechanteur, A.; Semdé, R.; Evrard, B. Pharmaceutical Approaches for Enhancing Solubility and Oral Bioavailability of Poorly Soluble Drugs. *Eur J Pharm Biopharm* **2024**, *204*, 114513.

59. Khan, K.U.; Minhas, M.U.; Badshah, S.F.; Suhail, M.; Ahmad, A.; Ijaz, S. Overview of Nanoparticulate Strategies for Solubility Enhancement of Poorly Soluble Drugs. *Life Sci* **2022**, *291*, 120301.
60. Csicsák, D.; Szolláth, R.; Kádár, S.; Ambrus, R.; Bartos, C.; Balogh, E.; Antal, I.; Köteles, I.; Tőzsér, P.; Bárdos, V.; Horváth, P.; Borbás, E.; Takács-Novák, K.; Sinkó, B.; Völgyi, G. The Effect of the Particle Size Reduction on the Biorelevant Solubility and Dissolution of Poorly Soluble Drugs with Different Acid-Base Character. *Pharmaceutics* **2023**, *15*, 15010278.
61. Cid-Samamed, A.; Rakmai, J.; Mejuto, J.C.; Simal-Gandara, J.; Astray, G. Cyclodextrins Inclusion Complex: Preparation Methods, Analytical Techniques and Food Industry Applications. *Food Chem* **2022**, *384*, 132467.
62. Porter, C.J.H.; Trevaskis, N.L.; Charman, W.N. Lipids and Lipid-Based Formulations: Optimizing the Oral Delivery of Lipophilic Drugs. *Nat Rev Drug Discov* **2007**, *6*, 231–248.
63. Sinkó B., Garrigues T.M., Balogh G.T., Nagy Z.K., Avdeef A., Takács-Novák K.: Skin-PAMPA: a new method for fast prediction of skin penetration. *Eur J Pharm Sci* **2012,** *45*, 698–707.
64. Sinkó, B.; Kökösi, J.; Avdeef, A.; Takács-Novák, K. A PAMPA Study of the Permeability-Enhancing Effect of New Ceramide Analogues. *Chem Biodivers* **2009**, *6(11)*, 1867-74
65. Shaikh, M.S.I.; Derle, N.D.; Bhamber, R. Permeability Enhancement Techniques for Poorly Permeable Drugs: A Review. *J Appl Pharm Sci* **2012**, *2*, 34–39.
66. Sugano, K.; Nabuchi, Y.; Machida, M.; Asoh, Y. Permeation Characteristics of a Hydrophilic Basic Compound across a Bio-Mimetic Artificial Membrane. *Int J Pharm* **2004**, *275*, 271–278.
67. Liu, C.-X.; Song, N.-N.; Zhang, S.-Y. Overview of Factors Affecting Oral Drug Absorption Asian Journal of Drug Metabolism and Pharmacokinetics Overview of Factors Affecting Oral Drug Absorption. *Asian J Drug Metab Pharmacokinet* **2004**, *4*, 167-176.
68. Seo, P.R.; Teksin, Z.S.; Kao, J.P.Y.; Polli, J.E. Lipid Composition Effect on Permeability across PAMPA. *Eur J Pharm Sci* **2006**, *29*, 259–268.

69. Seelig, A. The Role of Size and Charge for Blood-Brain Barrier Permeation of Drugs and Fatty Acids. *J Mol Neurosci* **2007**, *33*, 32–41.
70. Martinez, M.N.; Amidon, G.L. A Mechanistic Approach to Understanding the Factors Affecting Drug Absorption: A Review of Fundamentals. *J Clin Pharmacol* **2002**, *42*, 620–643.
71. Stuart, M.; Box, K. Chasing Equilibrium: Measuring the Intrinsic Solubility of Weak Acids and Bases. *Anal Chem* **2005**, *77*, 983–990.
72. Avdeef, A. pH-Metric Solubility. 1. Solubility-pH Plots. Gibbs Buffer and pKa Profiles from Bjerrum the Solid State. *Pharm Pharmacol Commun* **1998**; *4*;165-178.
73. Avdeef, A.; Berger, C.M. pH-Metric Solubility. 3. Dissolution Titration Template Method for Solubility Determination. *Eur J Pharm Sci* **2001**; 281-91.
74. Veseli, A.; Žakelj, S.; Kristl, A. A Review of Methods for Solubility Determination in Biopharmaceutical Drug Characterization. *Drug Dev Ind Pharm* **2019**, *45*, 1717–1724.
75. Tsinman, K.; Avdeef, A.; Tsinman, O.; Voloboy, D. Powder Dissolution Method for Estimating Rotating Disk Intrinsic Dissolution Rates of Low Solubility Drugs. *Pharm Res* **2009**, *26*, 2093–2100.
76. Faller, Bernard.; Urban, Laszlo. *Hit and Lead Profiling : Identification and Optimization of Drug-like Molecules*; Wiley-VCH, **2009**; ISBN 9783527323319.
77. Jacobsen, A.C.; Nielsen, S.; Brandl, M.; Bauer-Brandl, A. Drug Permeability Profiling Using the Novel Permeapad® 96-Well Plate. *Pharm Res* **2020**, *37*, 93.
78. Kabedev, A.; Tønning, M.H.; Teleki, A.; Bauer-Brandl, A.; Jacobsen, A.C. Understanding the Transport of Drugs across Biomimetic Barriers of Various Phospholipid Compositions Using a Combined Experimental and Computational Approach. *Colloids Surf B Biointerfaces* **2025**, *253*, 114706.
79. Sarmento, B.; Andrade, F.; Da Silva, S.B.; Rodrigues, F.; Das Neves, J.; Ferreira, D. Cell-Based in Vitro Models for Predicting Drug Permeability. *Expert Opin Drug Metab Toxicol* 2012, *8*, 607–621.
80. Volpe, D.A. Drug-Permeability and Transporter Assays in Caco-2 and MDCK Cell Lines. *Future Med Chem* **2011**, *3*, 2063–2077.

81. Kansy, M.; Senner, F.; Gubernator, K. Physicochemical High Throughput Screening: Parallel Artificial Membrane Permeation Assay in the Description of Passive Absorption Processes. *J Med Chem* **1998**, *41*, 7.

82. Di, L.; Kerns, E.H.; Fan, K.; McConnell, O.J.; Carter, G.T. High Throughput Artificial Membrane Permeability Assay for Blood-Brain Barrier. *Eur J Med Chem* **2003**, *38*, 223–232.

83. Avdeef, A. The Rise of PAMPA. *Expert Opin Drug Metab Toxicol* **2005**, *1*, 325–342.

84. Henriques, P.; Bicker, J.; Silva, S.; Doktorovová, S.; Fortuna, A. Nasal-PAMPA: A Novel Non-Cell-Based High Throughput Screening Assay for Prediction of Nasal Drug Permeability. *Int J Pharm* **2023**, *643*, 123252.

85. Dargó, G.; Vincze, A.; Müller, J.; Kiss, H.J.; Nagy, Z.Z.; Balogh, G.T. Corneal-PAMPA: A Novel, Non-Cell-Based Assay for Prediction of Corneal Drug Permeability. *Eur J Pharm Sci* **2019**, *128*, 232–239.

86. Vincze, A.; Dargó, G.; Balogh, G.T. Cornea-PAMPA as an Orthogonal in Vitro Physicochemical Model of Corneal Permeability. *Period Polytech Chem Eng* **2020**, *64*, 384–390.

87. Biondo, N.E.; Argenta, D.F.; Caon, T. A Comparative Analysis of Biological and Synthetic Skin Models for Drug Transport Studies. *Pharm Res* **2023**, *40*, 1209–1221.

88. Sugano, K.; Takata, N.; Machida, M.; Saitoh, K.; Terada, K. Prediction of Passive Intestinal Absorption Using Bio-Mimetic Artificial Membrane Permeation Assay and the Paracellular Pathway Model. *Int J Pharm* **2002**, *241*, 241-51.

89. Ottaviani, G.; Martel, S.; Carrupt, P.-A. Parallel Artificial Membrane Permeability Assay: A New Membrane for the Fast Prediction of Passive Human Skin Permeability. *J Med Chem* **2006**, *49*, 3948-54.

90. Sinkó, B.; Vizserálek, G.; Takács-Novák, K. Skin PAMPA: Application in Practice. *ADMET DMPK* **2014**, *2*, 191–198.

91. Soriano-Meseguer, S.; Fuguet, E.; Port, A.; Rosés, M. Optimization of Experimental Conditions for Skin-PAMPA Measurements. *ADMET DMPK* **2020**, *8*, 16–28.

92. Kumar, M.; Sharma, A.; Mahmood, S.; Thakur, A.; Mirza, M.A.; Bhatia, A. Franz Diffusion Cell and Its Implication in Skin Permeation Studies. *J Dispers Sci Technol* **2024**, *45*, 943–956.
93. Ng, S.F.; Rouse, J.J.; Sanderson, F.D.; Meidan, V.; Eccleston, G.M. Validation of a Static Franz Diffusion Cell System for in Vitro Permeation Studies. *AAPS Pharm Sci Tech* **2010**, *11*, 1432–1441.
94. Holzem, F.L.; Weck, A.; Schaffland, J.P.; Stillhart, C.; Klein, S.; Bauer-Brandl, A.; Brandl, M. Biopredictive Capability Assessment of Two Dissolution/Permeation Assays, MFLUX™ and PermeaLoop™, Using Supersaturating Formulations of Posaconazole. *Eur J Pharm Sci* **2022**, *176*, 106260.
95. Kádár, S.; Kennedy, A.; Lee, S.; Ruiz, R.; Farkas, A.; Tőzsér, P.; Csicsák, D.; Tóth, G.; Sinkó, B.; Borbás, E. Bioequivalence Prediction with Small-Scale Biphasic Dissolution and Simultaneous Dissolution-Permeation Apparatus—An Aripiprazole Case Study. *Eur J Pharm Sci* **2024**, *198*, 106782.
96. Borbás, E.; Balogh, A.; Bocz, K.; Müller, J.; Kiserdei, É.; Vigh, T.; Sinkó, B.; Marosi, A.; Halász, A.; Dohányos, Z.; Szente, L.; Balogh, Gy. T; Nagy, Zs. K.. In Vitro Dissolution-Permeation Evaluation of an Electrospun Cyclodextrin-Based Formulation of Aripiprazole Using MFlux™. *Int J Pharm* **2015**, *491*, 180–189.
97. Tőzsér, P.; Kovács, L.L.; Kádár, S.; Csicsák, D.; Sóti, P.; Völgyi, G.; Sinkó, B.; Nagy, Z.K.; Borbás, E. The Effect of Surfactants and pH Modifying Agents on the Dissolution and Permeation of Pimobendan. *Period Polytech Chem Eng* **2023**, *67*, 1–10.
98. Borbás, E.; Nagy, Z.K.; Nagy, B.; Balogh, A.; Farkas, B.; Tsinman, O.; Tsinman, K.; Sinkó, B. The Effect of Formulation Additives on in Vitro Dissolution-Absorption Profile and in Vivo Bioavailability of Telmisartan from Brand and Generic Formulations. *Eur J Pharm Sci* **2018**, *114*, 310–317.
99. Sironi, D.; Rosenberg, J.; Bauer-Brandl, A.; Brandl, M. PermeaLoop™ a Novel in Vitro Tool for Small-Scale Drug-Dissolution/Permeation Studies. *J Pharm Biomed Anal* **2018**, *156*, 247–251.

100. Dahan, A.; Beig, A.; Lindley, D.; Miller, J.M. The Solubility–Permeability Interplay and Oral Drug Formulation Design: Two Heads Are Better than One. *Adv Drug Deliv Rev* **2016**, *101*, 99–107.
101. Dahan, A.; Miller, J.M.; Hoffman, A.; Amidon, G.E.; Amidon, G.L. The Solubility-Permeability Interplay in Using Cyclodextrins as Pharmaceutical Solubilizers: Mechanistic Modeling and Application to Progesterone. *J Pharm Sci* **2010**, *99*, 2739–2749.
102. Beig, A.; Miller, J.M.; Lindley, D.; Carr, R.A.; Zocharski, P.; Agbaria, R.; Dahan, A. Head-To-Head Comparison of Different Solubility-Enabling Formulations of Etoposide and Their Consequent Solubility-Permeability Interplay. *J Pharm Sci* **2015**, *104*, 2941–2947.
103. Maher, S.; Geoghegan, C.; Brayden, D.J. Safety of Surfactant Excipients in Oral Drug Formulations. *Adv Drug Deliv Rev* **2023**, *202*, 115086.
104. Fine-Shamir, N.; Dahan, A. Solubility-Enabling Formulations for Oral Delivery of Lipophilic Drugs: Considering the Solubility-Permeability Interplay for Accelerated Formulation Development. *Expert Opin Drug Deliv* **2024**, *21*, 13–29.
105. Beig, A.; Agbaria, R.; Dahan, A. The Use of Captisol (SBE7-β-CD) in Oral Solubility-Enabling Formulations: Comparison to HPβCD and the Solubility-Permeability Interplay. *Eur J Pharm Sci* **2015**, *77*, 73–78.
106. Loftsson, T.; Brewster, M.E. Pharmaceutical Applications of Cyclodextrins: Effects on Drug Permeation through Biological Membranes. *J Pharm Pharmacol*, **2011**, *63*, 1119–1135.
107. Soe, H.M.S.H.; Maw, P.D.; Loftsson, T.; Jansook, P. A Current Overview of Cyclodextrin-Based Nanocarriers for Enhanced Antifungal Delivery. *Pharmaceuticals* **2022**, *15*, 1447.
108. Fine-Shamir, N.; Dahan, A. Ethanol-Based Solubility-Enabling Oral Drug Formulation Development: Accounting for the Solubility-Permeability Interplay. *Int J Pharm* **2024**, *653*, 123893.
109. Fine-Shamir, N.; Beig, A.; Miller, J.M.; Dahan, A. The Solubility, Permeability and the Dose as Key Factors in Formulation Development for Oral Lipophilic Drugs: Maximizing the Bioavailability of Carbamazepine with a Cosolvent-Based Formulation. *Int J Pharm* **2020**, *582*, 119307.

110. Hopkins Hatzopoulos, M.; Eastoe, J.; Dowding, P.J.; Rogers, S.E.; Heenan, R.; Dyer, R. Are Hydrotropes Distinct from Surfactants? *Langmuir* **2011**, *27*, 12346–12353.
111. Beig, A.; Lindley, D.; Miller, J.M.; Agbaria, R.; Dahan, A. Hydrotropic Solubilization of Lipophilic Drugs for Oral Delivery: The Effects of Urea and Nicotinamide on Carbamazepine Solubility-Permeability Interplay. *Front Pharmacol* **2016**, *7*, 379.
112. Schmaus G, V.G.J.K.F.H. 4-(1-Phenylethyl) 1,3-Benzenediol: A New Highly Potent Lightening Agent. *J Cosmet Sci* **2006**, *57*, 197–198.
113. Zhang, Y.; Sil, B.C.; Kung, C.P.; Hadgraft, J.; Heinrich, M.; Sinko, B.; Lane, M.E. Characterization and Topical Delivery of Phenylethyl Resorcinol. *Int J Cosmet Sci* **2019**, *41*, 479–488.
114. Fülöp F., Noszál. B., Szász. G., Takácsné Novák K. (szerk.) *Gyógyszerészi Kémia*; Semmelweis Kiadó: Budapest, **2010.**
115. Boyle, K.L.; Leech, E. A Review of the Pharmacology and Clinical Uses of Pimobendan. *JVECC* **2012**, *22*, 398–408.
116. Selzer, D.; Abdel-Mottaleb, M.M.A.; Hahn, T.; Schaefer, U.F.; Neumann, D. Finite and Infinite Dosing: Difficulties in Measurements, Evaluations and Predictions. *Adv Drug Deliv Rev* 2013, *65*, 278–294.
117. OECD Test No. 105: Water Solubility. In OECD Guidelines for the Testing of Chemicals, Section 1; Organisation for Economic Co-Operation and Development (OECD) **1995**.
118. Korinth, G.; Schaller, K.H.; Drexler, H. Is the Permeability Coefficient Kp a Reliable Tool in Percutaneous Absorption Studies? *Arch Toxicol* **2005**, *79*, 155–159.
119. Völgyi, G.; Csicsák, D.; Takács-Novák, K. Right Filter-Selection for Phase Separation in Equilibrium Solubility Measurement. *Eur J Pharm Sci* **2018**, *123*, 98–105.
120. R Core Team. *R: A Language and Environment for Statistical Computing*; Vienna, Austria, **2021**.
121. Hothorn T, B.F.W.P. Simultaneous Inference in General Parametric Models. *Biom J* **2008**, *50*, 346–363.

122. Pop, A.L.; Musuc, A.M.; Nicoară, A.C.; Ozon, E.A.; Crisan, S.; Penes, O.N.; Nasui, B.A.; Lupuliasa, D.; Secăreanu, A.A. Optimization of the Preformulation and Formulation Parameters in the Development of New Extended-Release Tablets Containing Felodipine. *Appl Sci* **2022**, *12*, 5333.
123. El-Massik, M.A.; Abdallah, O.Y.; Galal, S.; Daabis, N.A. Towards a Universal Dissolution Medium for Carbamazepine. *Drug Dev Ind Pharm* **2006**, *32*, 893–905.
124. Luo, L.; Patel, A.; Sinko, B.; Bell, M.; Wibawa, J.; Hadgraft, J.; Lane, M.E. A Comparative Study of the in Vitro Permeation of Ibuprofen in Mammalian Skin, the PAMPA Model and Silicone Membrane. *Int J Pharm* **2016**, *505*, 14–19.
125. Jain, P.; Goel, A.; Sharma, S.; Parmar, M. Solubility Enhancement Techniques with Special Emphasis on Hydrotrophy. *IJPPR* **2010**, *1*, 34-35.
126. Booth, J.J.; Abbott, S.; Shimizu, S. Mechanism of Hydrophobic Drug Solubilization by Small Molecule Hydrotropes. *J Phys Chem B* **2012**, *116*, 14915-21.
127. Dash, R.P.; Srinivas, N.R.; Babu, R.J. Use of Sorbitol as Pharmaceutical Excipient in the Present Day Formulations–Issues and Challenges for Drug Absorption and Bioavailability. *Drug Dev Ind Pharm* **2019**, *45*, 1421–1429.
128. Chen, M.L.; Straughn, A.B.; Sadrieh, N.; Meyer, M.; Faustino, P.J.; Ciavarella, A.B.; Meibohm, B.; Yates, C.R.; Hussain, A.S. A Modern View of Excipient Effects on Bioequivalence: Case Study of Sorbitol. *Pharm Res* **2007**, *24*, 73–80.
129. Volkova, T.; Simonova, O.; Perlovich, G. Mechanistic Insight in Permeability through Different Membranes in the Presence of Pharmaceutical Excipients: A Case of Model Hydrophobic Carbamazepine. *Pharmaceutics* **2024**, *16*, 184.
130. Medarević, D.; Kachrimanis, K.; Djurić, Z.; Ibrić, S. Influence of Hydrophilic Polymers on the Complexation of Carbamazepine with Hydroxypropyl-β-Cyclodextrin. *Eur J Pharm Sci* **2015**, *78*, 273–285.
131. Pal, A.; Roy, S.; Kumar, A.; Mahmood, S.; Khodapanah, N.; Thomas, S.; Agatemor, C.; Ghosal, K. Physicochemical Characterization, Molecular Docking, and in Vitro Dissolution of Glimepiride-Captisol Inclusion Complexes. *ACS Omega* **2020**, *5*, 19968–19977.

132. Li, M.; Qiao, N.; Wang, K. Influence of Sodium Lauryl Sulfate and Tween 80 on Carbamazepine-Nicotinamide Cocrystal Solubility and Dissolution Behaviour. *Pharmaceutics* **2013**, *5*, 508–524.
133. Fuguet, E.; Ràfols, C.; Rosés, M.; Bosch, E. Critical Micelle Concentration of Surfactants in Aqueous Buffered and Unbuffered Systems. *Anal Chim Acta* **2005**, *548*, 95–100.
134. Bhattachar, S.N.; Risley, D.S.; Werawatganone, P.; Aburub, A. Weak Bases and Formation of a Less Soluble Lauryl Sulfate Salt/Complex in Sodium Lauryl Sulfate (SLS) Containing Media. *Int J Pharm* **2011**, *412*, 95–98.
135. Sivakumar, P. Overview on Pharmaceutical Polymers. *WJPPS* **2021**, *10*, 953-975.
136. Bolten, D.; Lietzow, R.; Türk, M. Solubility of Ibuprofen, Phytosterol, Salicylic Acid, and Naproxen in Aqueous Solutions. *Chem Eng Technol* **2013**, *36*, 426–434.
137. Zhao, M.Y.; Shi, X.B.; Chang, J.H.; Wang, R.X.; Zhou, J.Y.; Liu, P. Amorphous Solid Dispersions of Glycyrrhetinic Acid: Using Soluplus, PVP, and PVPVA as the Polymer Matrix to Enhance Solubility, Bioavailability, and Stability. *AAPS Pharm Sci Tech* **2025**, *26*, 18.
138. Guo, M.; Wang, K.; Qiao, N.; Yardley, V.; Li, M. Investigating Permeation Behavior of Flufenamic Acid Cocrystals Using a Dissolution and Permeation System. *Mol Pharm* **2018**, *15*, 4257–4272.
139. Knopp, M.M.; Olesen, N.E.; Holm, P.; Langguth, P.; Holm, R.; Rades, T. Influence of Polymer Molecular Weight on Drug–Polymer Solubility: A Comparison between Experimentally Determined Solubility in PVP and Prediction Derived from Solubility in Monomer. *J Pharm Sci* **2015**, *104*, 2905–2912.
140. Fornells, E.; Fuguet, E.; Mañé, M.; Ruiz, R.; Box, K.; Bosch, E.; Ràfols, C. Effect of Vinylpyrrolidone Polymers on the Solubility and Supersaturation of Drugs; a Study Using the Cheqsol Method. *Eur J Pharml Sci* **2018**, *117*, 227–235.
141. Sun, Y.E.; Tao, J.; Zhang, G.G.Z.; Yu, L. Solubilities of Crystalline Drugs in Polymers: An Improved Analytical Method and Comparison of Solubilities of Indomethacin and Nifedipine in PVP, PVP/VA, and PVAc. *J Pharm Sci* **2010**, *99*, 4023–4031.

9. Bibliography of the candidate's publications

9.1. Publications relevant to the dissertation

I. Sinkó B.; Bárdos V.; Vesztergombi D.; Kádár S.; Malcsiner P.; Moustie A.; Jouy C.; Takács-Novák K.; Grégoire S. Use of an in vitro skin parallel artificial membrane assay (Skin-PAMPA) as a screening tool to compare transdermal permeability of model compound 4-phenylethyl resorcinol dissolved in different solvents. *Pharmaceutics* **2021,** *13(11),* 1758.

II. Bárdos V.; Szolláth R.; Tőzsér P.; Mirzahosseini A.; Sinkó B.; Angi R.; Takács-Novák K.: Study of the influence of pharmaceutical excipients on the solubility and permeability of BCS class II drugs. *Sci. Pharm.* **2025,** *93(2),* 19.

9.2. Other, not related publications

III. Csicsák D.; Szolláth R.; Kádár S.; Ambrus R.; Bartos C.; Balogh E.; Antal I.; Köteles I., Tőzsér P.; Bárdos V.; Horváth P.; Borbás E.; Takács-Novák K.; Sinkó B.; Völgyi G.: The effect of the particle size reduction on the biorelevant solubility and dissolution of poorly soluble drugs with different acid-base character. *Pharmaceutics* **2023,** *15(1),* 278.

IV. Angi R.; Kalóczkai A. J.; Kovács A.; Marton A.; Bárdos V.; Dormán P.; Katona G.; Agócs A.; Csorba A., Nagy Z. Zs.; Vincze A.; Balogh G. T.: Harnessing cyclodextrins for enhanced ocular delivery of carotenoid derivatives: from development to ex vivo characterization. *Carbohydr. Polym. Tech. Appl.* **2025,** *9,* 100718.

V. Szolláth R.; Bárdos V.; Stifter-Mursits M.; Angi R.; Mazák K.: Effects of Different Centrifugation Parameters on Equilibrium Solubility Measurements. *Methods Protoc.* **2025***, 8,* 116.

VI. Takácsné Novák K.; Bárdos V.: A COPD kezelésében alkalmazott hosszú hatású hörgtágítók gyógyszerészi kémiai áttekintése. *Gyógyszerészet* **2020,** *64,* 8-14.

10. Acknowledgements

First of all. I am extremely grateful to Professor Krisztina Takács-Novák for her patience, persistent support and valuable advice, thanks to which I have gained invaluable knowledge and experience. I am also thankful to Gergely Völgyi (my former co-supervisor) for supporting and guiding my work with his advice, and to Réka Angi (my current co-supervisor) whose assistance allowed me to learn to analyse things from a different perspective.

I am thankful to Péter Horváth, former director of the Department of Pharmaceutical Chemistry, for making it possible for me to begin my PhD work here, and to György Tibor Balogh, the current director of the Department of Pharmaceutical Chemistry, for his mentorship and for inspiring me with his extensive knowledge.

I am thankful to Bálint Sinkó for supporting my work with his advice.

I am grateful to Szabina Madarász-Kádár, for helping me learn the correct method for conducting experiments and evaluate results at the beginning of my work, and for showing endless patience towards me.

I especially appreciate Petra Tőzsér, Rita Szolláth, and Balázs Simon for their advices, English language corrections, and continuous support throughout my work.

I am also thankful for the support of my professors and colleagues in the Department of Pharmaceutical Chemistry.

Finally, I wish to thank my family and friends, especially Martina, Zsuzsa, and Lindus, for their unwavering encouragement throughout my PhD work.